

This is the Preprint Version of the following article: *Aaron J. Martin & Howell Bosbyshell (2019). Further detrital zircon evidence for peri-Gondwanan blocks in the central Appalachian Piedmont Province, USA. Canadian Journal of Earth Sciences, 56, 1061-1076.*

To access the final edited and published work is available online at:
<https://doi.org/10.1139/cjes-2018-0253>

Martin and Bosbyshell, 2018, Central Appalachian Exotic Terranes

1 Further detrital zircon evidence for peri-Gondwanan blocks in the central Appalachian

2 Piedmont Province, USA

3

4 Aaron J. Martin¹, Howell Bosbyshell²

5

6 ¹División de Geociencias Aplicadas, IPICYT, CP 78216, San Luis Potosí, S.L.P.,

7 MEXICO. aaron.martin@ipicyt.edu.mx

8 Martin is corresponding author.

9 ²Earth and Space Sciences Department, West Chester University, West Chester, PA 19383

10 USA. HBosbyshell@wcupa.edu

11

12 Keywords: zircon, radiogenic isotopes, Appalachians, exotic terrane, orogeny

Draft

13 **0. ABSTRACT**

14 Evidence for exotic terranes in the central Appalachian Piedmont Province is
15 fragmented between central Virginia, northern Maryland, and southeastern Pennsylvania.
16 Here we present LA-ICPMS data from detrital zircon that supports the presence of an
17 exotic terrane in this region. U/Pb dating of detrital zircon from new samples of the Storck
18 quartzite (central Virginia) and the Hoods Mill rocks (northern Maryland) confirms the
19 presence of a major age peak at ca. 630-610 Ma in these units. These ages are consistent
20 with derivation from Gondwana, but not Ediacaran Laurentia. Further, modern ϵ_{Hf} values
21 of five of the ca. 670-580 Ma grains in these samples are inconsistent with derivation from
22 the few plutons of this age in Ediacaran Laurentia. The Loch Raven Schist and a
23 sedimentary xenolith in the Wilmington Complex contain a smaller proportion of ca. 670-
24 580 Ma grains than the Storck quartzite and the Hoods Mill rocks, but more such grains
25 than in sediment derived from Ediacaran Laurentia, so we tentatively conclude that these
26 two units also received sediment from Gondwana. Detrital zircon ages from the type
27 localities of the Piney Run Formation, Pleasant Grove Schist, Prettyboy Schist, and
28 Wissahickon Formation indicate sediment provenance in Ediacaran Laurentia. We also
29 present new U-Pb and Lu-Hf isotopic data from western Newfoundland plutons for
30 comparison with such data from the detrital zircon. Intrusion ages of the Steel Mountain
31 Anorthosite, Disappointment Hill Tonalite, and Round Pond Granite are 608 ± 12 , 600 ± 8 ,
32 and 590 ± 9 Ma, respectively. None of these units was derived entirely from the depleted
33 mantle.

34 1. INTRODUCTION

35 Successive accretion of magmatic arcs and ribbon continents to the eastern margin
36 of Laurentia during Early Ordovician to Early Mississippian time caused pulses of orogeny
37 in eastern Laurentia (van Staal et al., 2009; Pollock et al., 2012; Hibbard et al., 2012). In
38 the northern and southern Appalachian Orogen, many of these accreted terranes were exotic
39 to Laurentia, originally derived from the edges of Gondwana (Fig. 1; Pollock et al., 2012;
40 Macdonald et al., 2014). In the central Appalachian Piedmont Province, Early Ordovician
41 to Late Devonian deformation and metamorphism were widespread and locally intense
42 (Drake, 1989; Bosbyshell et al., 1999; 2016; Kunk et al., 2005; Aleinikoff et al., 2006;
43 Wintsch et al., 2010; Hughes et al., 2013), yet geologists have found only fragmentary
44 evidence for terranes derived from Gondwana.

45 The strongest published evidence for continental crust with Gondwanan affinity in
46 the central Appalachian Orogen consists of U/Pb isotopic ages of detrital zircon from
47 Cambrian-Ordovician meta-sandstone samples taken from three Piedmont Province
48 localities (Fig. 2; Hughes et al., 2014; Bosbyshell et al., 2015; Martin et al., 2015). The
49 three sample locations are in central Virginia (1 sample), northern Maryland (1 sample),
50 and southeastern Pennsylvania (4 samples). Some of the detrital zircon U/Pb ages from
51 these samples are not easily explained as originating from Ediacaran Laurentia but are
52 consistent with sediment derivation from a Gondwanan source. Most cogently, the
53 existence of abundant ages between 670 and 580 Ma in all these samples suggests
54 Gondwanan provenance. The 670-580 Ma ages are significant because felsic magmatism
55 of this age is known from only two locations in probable Ediacaran Laurentia. The
56 Goochland Terrane of central Virginia contains several small granitic plutons with
57 crystallization ages between ca. 660 and 580 Ma (Owens and Tucker, 2003), and several

Martin and Bosbyshell, 2018, Central Appalachian Exotic Terranes

58 granitic plutons in western Newfoundland crystallized between ca. 630 and 590 Ma
59 (Williams et al., 1985; van Berkel and Currie, 1988; Currie et al., 1992; Lin et al., 2013).
60 Further evidence for a Gondwanan sediment source to the sampled sandstone includes the
61 following two considerations. First, in some samples there is an absence of a spike in ages
62 at ca. 1200-950 Ma, the presence of which is a distinctive feature of Laurentia-derived
63 sediment deposited on the eastern margin of the continent (e.g., Macdonald et al., 2014,
64 Hughes et al., 2014; Martin et al., 2015). Second, some detrital zircon grains yielded U/Pb
65 ages between 950 and 780 Ma, which also was a period of scarce metamorphism or felsic
66 magmatism in Laurentia (Whitmeyer and Karlstrom, 2007). Bailey et al. (2008) reported
67 detrital zircon U/Pb ages between 950 and 780 Ma from a sandstone from central Virginia,
68 and likewise concluded that there was a Gondwanan sediment source to this sandstone
69 (Shores melange sample shown in Hughes et al., 2014). The existence of only a few meta-
70 sandstone samples with an apparent Gondwanan detrital zircon U/Pb age signature, and the
71 100 km that separates each of the central Virginia, northern Maryland, and southeastern
72 Pennsylvania sample localities, challenges secure recognition and reconstruction of a
73 putative peri-Gondwanan terrane in the Piedmont of the central Appalachian Orogen.

74 This paper investigates the possible presence of a Gondwana-derived terrane in the
75 central Appalachian Piedmont Province using a three-pronged approach. First, we confirm
76 the existence of sandstone that contains detrital zircon with a Gondwanan U/Pb age
77 signature by dating detrital zircon from new samples collected near the sites of the first
78 discoveries in central Virginia and northern Maryland (Hughes et al., 2014; Martin et al.,
79 2015). Second, we test whether the 670-580 Ma detrital zircon is incompatible with
80 derivation from Ediacaran Laurentia by comparing Hf isotope values in spots in the detrital
81 zircon grains to Hf isotope values in spots in zircon from the two possible Laurentian

Martin and Bosbyshell, 2018, Central Appalachian Exotic Terranes

82 sources, the granitoid in the Goochland Terrane and western Newfoundland. Third, we
83 search for more locations in the central Appalachian Piedmont Province that expose
84 sandstone with Gondwanan detrital zircon U/Pb age signatures.

85

86 **2. TECTONIC SETTING**

87 The Appalachian Orogen was part of a larger system of orogens that formed on the
88 eastern edge of Laurentia during the Paleozoic Era (Scotese and Langford, 1995; Pollock et
89 al., 2012). Geologists apply the term “Appalachian” to the portion of this larger orogen in
90 the eastern United States and Canada between Alabama and Newfoundland (Fig. 1;
91 Hibbard et al., 2006). In this article, we treat the southern Appalachians as that part of the
92 orogen southwest of the northeastern limit of Carolina in central Virginia, the northern
93 Appalachians as the sector northeast of the southernmost exposure of Ganderia in southern
94 Connecticut, and the central Appalachians as the portion between the northeastern limit of
95 Carolina and the southernmost exposures of Ganderia (Fig. 1).

96 Geologists use distinctions originally based on physiography to divide the central
97 and southern Appalachian Orogen into four tectonic provinces (Hatcher, 1989). From west
98 to east these are the Valley and Ridge, Blue Ridge, Piedmont, and Coastal Plain provinces.
99 The focus of this article is the Piedmont Province. Dominated by metasedimentary rocks,
100 the Piedmont Province is the formerly deepest and most outboard part of the orogen
101 currently exposed (Hibbard et al., 2006). Meta-volcanic, meta-plutonic, and
102 unmetamorphosed plutonic rocks also are present, particularly in eastern parts of the
103 Piedmont Province (Hibbard et al., 2006). Deposition and intrusion mostly occurred during
104 the Neoproterozoic and Paleozoic eras (Reinhardt, 1974; 1977; Fisher et al., 1979;
105 Aleinikoff et al., 2002; 2006; Owens and Tucker, 2003; Horton et al., 2010; Owens et al.,

Martin and Bosbyshell, 2018, Central Appalachian Exotic Terranes

106 2010; Pollock et al., 2010; Hughes et al., 2013; 2014; Bosbyshell et al., 2015; Martin et al.,
107 2015). Piedmont Province rocks constitute a collage of fault-bounded terranes of varying
108 origin (Fig. 2; Horton et al., 1989). The rocks in some terranes, such as the Westminster
109 Terrane and most of the Potomac Terrane, intruded or were deposited on the eastern edge
110 of Laurentia (Hughes et al., 2014; Martin et al., 2015). Others, such as the Carolina
111 Domain, intruded and were deposited on the periphery of Gondwana (Pollock et al., 2012).
112 The depositional or intrusive origins of a few continental blocks are debated; examples
113 include the Goochland Terrane and the Wilmington Complex and adjacent rocks (Farrar,
114 1984; Horton et al., 1989; Glover et al., 1997; Aleinikoff et al., 2006; Bosbyshell et al.,
115 2015).

116 Geologists have assigned many names to and used shifting criteria to group the
117 metasedimentary rocks of the Piedmont Province in the central Appalachian Orogen over
118 the past 130 years (Williams, 1891; 1892; Bascom, 1902; 1905; Mathews, 1904; 1905;
119 Mathews and Grasty, 1909; Knopf and Jonas, 1923; Virginia Geological Survey, 1928;
120 Jonas and Stose, 1938; Hopson, 1964; Southwick and Fisher, 1967; Rodgers, 1970;
121 Higgins, 1972; Crowley, 1976; Horton et al., 1989; Hibbard et al., 2006; Southworth et al.,
122 2007; Bosbyshell et al., 2015; Martin et al., 2015). Neither detrital zircon U/Pb ages nor
123 other provenance indicators were used in the assignments prior to approximately 2006.
124 More recent U/Pb isotopic dating of detrital zircon made clear that some of the classical
125 lithology-based correlations and groupings are not supported by the new dating (Hughes et
126 al., 2014; Bosbyshell et al., 2015; Martin et al., 2015). It is beyond the scope of this article
127 to discuss the history of formation names or to provide a resolution to naming conflicts in
128 the central Appalachian Piedmont Province. Instead, we show sample locations in Figure 2
129 free of the biases produced by the old lithology-based formation names. In Table 1 we list

Martin and Bosbyshell, 2018, Central Appalachian Exotic Terranes

130 the formation names as currently applied but emphasize that in some cases these formation
131 names are not compatible with recent studies of detrital zircon U/Pb ages. One of the
132 samples listed in Table 1 came from a metasedimentary xenolith in the Brandywine Blue
133 Gneiss, which is a member of the Wilmington Complex. The Wilmington Complex is an
134 Early Ordovician island arc metamorphosed to granulite facies during the Silurian Period
135 (Aleinikoff et al., 2006).

136 From west to east, the island of Newfoundland consists of a Laurentian/peri-
137 Laurentian domain and two peri-Gondwanan domains, Ganderia and Avalonia. Cawood et
138 al. (1995) divided part of the Laurentian domain into several fault-bounded tectonic blocks
139 with partially distinct geologic histories. Two of our Newfoundland samples come from a
140 central block, the Corner Brook Lake block (Fig. 3; Table 2). In the Corner Brook Lake
141 block, the oldest rocks are granulite facies gneiss and related rocks with protolith igneous
142 crystallization ages of ca. 1500 Ma (Currie et al., 1992; Cawood et al., 1996; Lin et al.,
143 2013). These Mesoproterozoic units were intruded by a suite of granitic magmas at ca. 600
144 Ma (Williams et al., 1985; van Berkel and Currie, 1988; Currie et al., 1992; Lin et al.,
145 2013) as well as by bimodal magmas at ca. 555 Ma (Cawood et al., 1995). Our third
146 Newfoundland sample comes from the Steel Mountain Anorthosite, which intruded the
147 Mesoproterozoic Corner Brook Lake rocks in some locations and was thrust below the
148 southern edge of the Corner Brook Lake block in others (Fig. 3; Lin et al., 2013). The
149 intrusion age of the Steel Mountain Anorthosite heretofore was assumed to be
150 Mesoproterozoic (Lin et al., 2013) but in this contribution is shown to be ca. 608 Ma. The
151 Proterozoic rocks are unconformably overlain by Ediacaran to Ordovician clastic and
152 carbonate deposits (Cawood and Nemchin, 2001). Lin et al. (2013) concluded that the
153 Corner Brook Lake block, traditionally held to be the para-autochthonous former eastern

Martin and Bosbyshell, 2018, Central Appalachian Exotic Terranes

154 margin of Laurentia, is in fact allochthonous, placed in its present position by motion on
155 Paleozoic transcurrent faults.

156 Laurentia consisted of an Archean nucleus surrounded by Proterozoic and Paleozoic
157 terranes, some of which originated far from Laurentia (Whitmeyer and Karlstrom, 2007).
158 Regardless of their origin, after accretion to the continent these terranes became part of
159 Laurentia. We therefore consider a Laurentian sediment source to be a source in Laurentia
160 as the continent existed at the time of deposition. The sedimentary rocks considered in this
161 article were deposited during or after the Ediacaran Period, so we refer to the continent as
162 Ediacaran Laurentia when discussing sediment provenance. We use modern orientations to
163 indicate compass directions, though it is important to consider that Laurentia rotated in map
164 view during the Neoproterozoic and Paleozoic eras (Li et al., 2008; Pollock et al., 2012).
165 Previous authors have referred to named high strain zones using the term “fault” or “shear
166 zone” without careful attention to deformation mechanisms in some cases. We retain the
167 historical uses of these words to ease comparison with previous publications and because
168 deformation mechanisms are irrelevant for the conclusions in this article.

169

170 **3. METHODS**

171 **3.1 Sample collection and zircon processing**

172 Martin collected all samples. Each meta-sandstone sample came from the least
173 micaceous, coarsest-grained part of the outcrop. Photomicrographs of thin sections from
174 every sample are shown in Figure S1.

175 Martin et al (2015) reported Gondwanan zircon in a meta-sandstone in the Mather
176 Gorge Formation of northern Maryland. In this paper we assign the informal name “Hoods
177 Mill rocks” to these exotic rocks because their provenance is distinct from that of the

Martin and Bosbyshell, 2018, Central Appalachian Exotic Terranes

178 Mather Gorge Formation near its type section, which was derived from Ediacaran
179 Laurentia. For the current paper, Martin collected a new sample of the Hoods Mill rocks to
180 verify the presence of Gondwanan detrital zircon (Table 1). The new sample was collected
181 south of the south branch of the Patapsco River and east of Maryland State Route 97
182 whereas the sample reported in Martin et al. (2015) was located along the railroad tracks
183 north of the river and directly west of the road. For the same purpose, Martin collected a
184 new sample of the informally-named Storck quartzite of central Virginia near the location
185 of the sample with Gondwanan zircon described by Hughes et al. (2014).

186 Zircon was separated and mounted in the laboratories in the Department of Geology
187 at the University of Maryland. We isolated zircon from each sample by first crushing the
188 rock using a mortar and pestle, then removing silt- and clay-sized particles by hand-panning
189 in water, removing magnetic grains with a Frantz magnetic barrier separator, and removing
190 less-dense grains in methylene iodide. We poured the now nearly-pure zircon onto double-
191 sided tape and cast the grains in an epoxy disk together with shards or loose grains of
192 reference zircon crystals. We then sanded and polished the disks by hand to expose the
193 interiors of the grains. Prior to isotopic analysis, we imaged the grains using backscattered
194 electrons and cathodoluminescence in the JEOL JXA-8900R electron probe microanalyzer
195 at the University of Maryland. The images were used to avoid multiple
196 cathodoluminescence zones, cracks, and inclusions during selection of spots for isotopic
197 analysis.

198

199 **3.2 Zircon mass spectrometry**

200 Zircon from the western Newfoundland igneous rocks and all central Appalachian
201 Piedmont Province meta-sandstone was analyzed in the Arizona LaserChron Center at the

Martin and Bosbyshell, 2018, Central Appalachian Exotic Terranes

202 University of Arizona (Tables 1 and 2). Gehrels and Pecha (2014), Pullen et al. (2014), and
203 Ibanez-Mejia et al. (2015) described the analytical procedures in detail; in this sub-section
204 we briefly summarize these methods. We first analyzed spots in zircon grains for uranium
205 and lead isotopes. We then selected zircon from samples 314002 (Storck quartzite) and
206 1213002 (Hoods Mill rocks) for in situ analysis of lutetium and hafnium isotopes in a
207 different analysis session. We focused on grains from these samples with ages between ca.
208 670 and 580 Ma; we also analyzed some younger and older grains. The laser spot for the
209 hafnium isotopic analyses was centered on the pit excavated by laser ablation for the
210 uranium and lead isotope measurements. All uncertainties are reported at the 2-sigma
211 level.

212

213 **3.2.1 Uranium-lead isotope measurements**

214 A 20 μm -diameter spot was ablated in each zircon grain using a Photon Machines
215 Analyte G2 excimer laser equipped with a HelEx ablation cell. The ablated zircon was
216 carried in helium into the plasma source of a Thermo Element2 single-collector high
217 resolution inductively coupled plasma mass spectrometer, which sequences rapidly through
218 measurement of U, Th, and Pb isotopes. Each analysis consisted of 5 s of background
219 measurement on peaks with the laser off, 10 s with the laser firing, and a 20 s delay to
220 purge the previous sample and save files. The resulting ablation pits were approximately
221 12 μm deep. Analyses of reference zircon FC52 and SL bracketed every 5 analyses of
222 sample zircon; these analyses were used to correct fractionation of the $^{206}\text{Pb}/^{207}\text{Pb}$ and
223 $^{206}\text{Pb}/^{238}\text{U}$ ratios, respectively. We also bracketed every 15 analyses of sample zircon with
224 an analysis of reference zircon R33, treated as an unknown in this situation, to check the

Martin and Bosbyshell, 2018, Central Appalachian Exotic Terranes

225 age determinations. Accepted ages for these standards are 1098.47 ± 0.16 , 563.5 ± 3.2 , and
226 420.53 ± 0.16 Ma for FC, SL, and R33, respectively (Gehrels et al., 2008; Mattinson, 2010).

227 Data reduction was performed offline using an in-house Python decoding routine
228 and an Excel program. Data reduction included the following steps. (1) Using the natural
229 isotopic ratio $^{202}\text{Hg}/^{204}\text{Hg} = 4.3$, subtraction of the contribution from ^{204}Hg to the mass 204
230 signal to yield ^{204}Pb intensity. This mercury correction was not significant for most
231 analyses because the mercury backgrounds were low. (2) Correction for common lead
232 based on the measured ratio $^{206}\text{Pb}/^{204}\text{Pb}$ and the assumed composition of common lead from
233 Stacey and Kramers (1975). (3) Correction for mass fractionation during analysis using the
234 bracketing analyses of the reference zircon. (4) Calculation of U and Th concentrations
235 using the measured intensity and known concentrations of reference zircon FC52. For
236 detrital grains, we removed from consideration analyses with greater than 20% normal
237 discordance, greater than 5% reverse discordance, or greater than 10% measurement
238 (internal) uncertainty. We used $^{206}\text{Pb}/^{238}\text{U}$ dates for grains with $^{206}\text{Pb}/^{207}\text{Pb}$ dates younger
239 than 900 Ma and $^{206}\text{Pb}/^{207}\text{Pb}$ dates for older grains.

240

241 **3.2.2 Lutetium-hafnium isotope measurements**

242 All Lu-Hf isotope data reported in this paper were acquired during a single analysis
243 session. We used a Nu multi-collector high resolution inductively coupled plasma mass
244 spectrometer to analyze hafnium isotopes. Instrument settings were established first by
245 measurements of 10 ppb solutions of JMC475 and a Spex Hf solution followed by
246 measurements of 10 ppb solutions containing Spex Hf, Yb, and Lu. These mixtures
247 contained a range of concentrations of Yb and Lu, with $^{176}(\text{Yb}+\text{Lu})$ up to 70% of the ^{176}Hf .
248 After instrument tuning using the solutions, the settings on the mass spectrometer were

Martin and Bosbyshell, 2018, Central Appalachian Exotic Terranes

249 optimized for laser ablation by a Photon Machines Analyte G2 excimer laser with a beam
250 diameter of 40 μm . We then analyzed shards or loose grains of seven different zircon
251 standards (R33, Temora, Mud Tank, Plesovice, 91500, FC52, and Sri Lanka) that were
252 included in the epoxy disks with the sample zircon. After precision and accuracy were
253 acceptable, we began analysis of zircon grains from the Appalachian samples using the
254 same acquisition parameters. Each analysis consisted of background measurement via a
255 single 40-second integration on peaks with the laser off followed by sixty 1-second
256 integrations with the laser firing. The ablation rate was about 0.8 μm per second. Analysis
257 of each standard bracketed about 20 analyses of sample zircon.

258 Data reduction was performed offline using an Excel program developed at the
259 Arizona LaserChron Center. We corrected for mass fractionation during analysis following
260 the method of Woodhead et al. (2004). All corrections were performed line-by-line. For
261 each 60-second analysis, the mean and standard error of the ratio $^{176}\text{Hf}/^{177}\text{Hf}$ were
262 calculated from the 1-second integrations after removing values more than two standard
263 deviations from the mean. We calculated the ratio $^{176}\text{Hf}/^{177}\text{Hf}$ at the time of zircon
264 crystallization using the measured $^{176}\text{Hf}/^{177}\text{Hf}$ and $^{176}\text{Lu}/^{177}\text{Hf}$ values and the ^{176}Lu decay
265 constant of $1.867 \times 10^{-11} \text{ year}^{-1}$ (Scherer et al., 2001; Soderlund et al., 2004).

266

267 **3.3 Uranium-lead data analysis and presentation**

268 We prepared concordia, weighted mean, and relative age-probability diagrams using
269 Isoplot version 4.15 (Ludwig, 2008). The weighted means were calculated with weighting
270 according to the square of the internal uncertainties. The total uncertainty on the intrusion
271 age determination for each western Newfoundland igneous sample was calculated by
272 quadratic addition of the measurement (internal) and systematic (external) uncertainties.

Martin and Bosbyshell, 2018, Central Appalachian Exotic Terranes

273 Age-probability diagrams for individual meta-sandstone samples show the age of each
274 dated zircon and its measurement error as a normal distribution, summed into a single
275 curve. Stacked age-probability plots from multiple meta-sandstone samples were prepared
276 using an Excel program written at the Arizona LaserChron Center. This program
277 normalizes the age-probability curves according to the number of constituent analyses such
278 that each curve contains the same area, allowing direct comparison of multiple datasets,
279 each composed of different numbers of analyses.

280

281 **3.4 Determination of maximum depositional ages**

282 Calculation of the maximum possible depositional age of a metasedimentary rock
283 using its youngest detrital zircon grains commonly is complicated by lead loss, growth of
284 metamorphic zircon, multiple age zones in a single grain, analytical error, and dating a very
285 small fraction of the total zircon present in the sedimentary rock. Using the youngest single
286 age from a set of detrital zircon U/Pb isotopic ages can result in a determination of
287 maximum depositional age that is younger than the true depositional age (Dickinson and
288 Gehrels, 2009). Instead, determining maximum depositional age using multiple analyses
289 that overlap within uncertainty yields a more robust constraint on the maximum possible
290 depositional age (Dickinson and Gehrels, 2009). We therefore calculate the maximum
291 depositional age as the weighted mean of the two or more youngest analyses that overlap at
292 the 1-sigma level plus the 2-sigma error on this weighted mean, rounded up to the nearest
293 10 M.y. interval.

294

295 **4. WESTERN NEWFOUNDLAND IGNEOUS ZIRCON SPOT U-PB AND LU-HF**

296 **ISOTOPE DATA**

Martin and Bosbyshell, 2018, Central Appalachian Exotic Terranes

297 **4.1 Western Newfoundland zircon U-Pb isotope data**

298 We placed one 20 μm -diameter analysis spot in each zircon crystal because most
299 crystals were small and many contained only one cathodoluminescence domain (Fig. 4).
300 Table S1 and figure 5 present the results of these analyses. The dates of the standard zircon
301 analyzed along with the unknowns mostly overlap the accepted ages within uncertainty
302 (Table S2).

303 Analyses of spots in 50 zircon crystals from sample 1013002 produced $^{206}\text{Pb}/^{238}\text{U}$
304 ages between 627 and 581 Ma (Table S1, Figs. 4, 5). Analyses of spots in 16 zircon grains
305 from sample 1013005 mostly yielded $^{206}\text{Pb}/^{238}\text{U}$ ages between 634 and 590 Ma plus one
306 concordant analysis with a $^{206}\text{Pb}/^{207}\text{Pb}$ age of ca. 1140 Ma (Table S1, Figs. 4, 5). Spot
307 analysis of 46 crystals from sample 1013006 yielded $^{206}\text{Pb}/^{238}\text{U}$ ages from 657 to 440 Ma
308 (Table S1, Figs. 4, 5). Several of these grains are discordant with $^{206}\text{Pb}/^{207}\text{Pb}$ ages between
309 ca. 1429 and 713 Ma.

311 **4.2 Western Newfoundland zircon Lu-Hf isotope data**

312 Repeated analysis of the seven zircon standards throughout the data acquisition
313 session yielded the following weighted mean values of the measured $^{176}\text{Hf}/^{177}\text{Hf}$ ratios.
314 R33: 0.282751 ± 6 , Temora: 0.282668 ± 7 , Mud Tank: 0.282540 ± 5 , Plesovice: 0.282500 ± 6 ,
315 91500: 0.282316 ± 7 , FC52: 0.282179 ± 6 , Sri Lanka: 0.281684 ± 5 (Fig. S2). These values
316 mostly overlap the accepted values within uncertainty; note, however, that different articles
317 report different values for some of the standards (Woodhead and Hergt, 2005; Kemp et al.,
318 2006; Slama et al., 2008; Fisher et al., 2014).

319 In order to fit the 40 μm -diameter laser spot into a single cathodoluminescence
320 domain while avoiding large cracks and inclusions, we were forced to analyze some

Martin and Bosbyshell, 2018, Central Appalachian Exotic Terranes

321 slightly discordant zircon (Tables S1, S3). Analysis of fifteen spots in zircon from sample
322 1013002 of the Disappointment Hill Tonalite yielded a range of current ϵ_{Hf} values between
323 -13.0 and -16.5 (Fig. 6; Table S3). This range was +0.2 to -3.6 at the time of intrusion, ca.
324 600 Ma. Analysis of five spots in non-xenocrystic zircon from sample 1013005 of the Steel
325 Mountain Anorthosite gave present-day ϵ_{Hf} values from -10.4 to -13.7 (Fig. 6; Table S3).
326 At 600 Ma, these values were +2.8 to -0.6. The modern ϵ_{Hf} value of the ca. 1140 Ma
327 crystal from sample 1013005 is -15.7; this value was +9.3 at 1140 Ma. The current ϵ_{Hf}
328 values of eight spots in non-xenocrystic zircon from sample 1013006 of the Round Pond
329 Granite ranges from -7.8 to -12.2; these values were +5.1 to -0.1 at 600 Ma (Fig. 6; Table
330 S3). These eight spots do not include the analysis from grain 31, which may be a xenocryst
331 (see section 6.1). Including the analysis of this grain would not change our interpretation
332 because its modern ϵ_{Hf} value of -7.9 falls within the range of ϵ_{Hf} values from the non-
333 xenocrystic zircon extracted from sample 1013006.

334

335 **5. CENTRAL APPALACHIAN PIEDMONT DETRITAL ZIRCON U-PB AND LU-** 336 **HF ISOTOPE DATA**

337 **5.1 Central Appalachian Piedmont detrital zircon U-Pb isotope data**

338 We placed one 20 μm -diameter analysis spot in each zircon grain. Table S4
339 contains the U-Pb isotope data from these spots and Figure S3 shows the ages in histograms
340 and relative probability plots. For analysis of Lu-Hf isotopes in zircon from samples
341 314002 and 1213002, we were forced to use six 5-16% reversely discordant analyses in
342 order to fit the 40 μm -diameter laser spot into the zircon grains without intersecting
343 multiple cathodoluminescence domains or large cracks or inclusions. These six U-Pb
344 isotope analyses are listed in red in Table S4. We used these spots only for the Lu-Hf

Martin and Bosbyshell, 2018, Central Appalachian Exotic Terranes

345 isotope analyses, we did not use the U-Pb isotope analyses for determination of sediment
346 provenance or maximum depositional ages. The mean ages of the zircon standards
347 analyzed with each sample overlap the accepted ages within uncertainty (Table S2).

348 Zircon from sample 314002 of the Storck quartzite (formal name: Mine Run
349 Complex I) yielded 269 analyses with ages between ca. 3064 and 499 Ma. Similarly,
350 zircon from sample 1213002 of the Hoods Mill rocks (formal name: Mather Gorge
351 Formation) produced 252 analyses with ages between ca. 3034 and 521 Ma.

352 194 analyses of zircon in sample 1213003 of the Loch Raven Schist yielded ages
353 from ca. 1801 to 397 Ma and one age of ca. 2601 Ma. Many grains younger than
354 approximately 460 Ma had high U/Th ratios, up to 380 (Table S4). Zircon from sample
355 114002 of the Piney Run Formation yielded 166 analyses with ages between ca. 2775 and
356 1033 Ma plus one analysis at ca. 514 Ma (167 analyses total). Sample 114003 of the
357 Pleasant Grove Schist yielded 271 ages between ca. 3005 and 955 Ma plus one analysis at
358 ca. 629 Ma and one at ca. 518 Ma (273 analyses total). Analyses of zircon from sample
359 314001 of the Prettyboy Schist yielded 284 ages from ca. 1915 to 910 Ma plus additional
360 ages at ca. 2478, 561, and 536 Ma (287 analyses total). 245 analyses in zircon from sample
361 314003 of the sedimentary xenolith in the Brandywine Blue Gneiss yielded ages between
362 ca. 1993 and 423 Ma. Finally, zircon from sample 114005 of the Wissahickon Formation
363 yielded 207 analyses with ages from ca. 2848 to 939 Ma plus two analyses at ca. 540 Ma
364 (209 analyses total).

365

366 **5.2 Central Appalachian Piedmont detrital zircon Lu-Hf isotope data**

367 We analyzed spots in 40 zircon grains from sample 314002 of the Storck quartzite
368 with crystallization ages between ca. 927 and 513 Ma (Tables 1; S3). The range of present-

Martin and Bosbyshell, 2018, Central Appalachian Exotic Terranes

369 day ϵ_{Hf} values in these crystals is -4 to -27 (Fig. 7, Table S3). We analyzed spots in 22
370 crystals from sample 1213002 of the Hoods Mill rocks with crystallization ages between ca.
371 911 and 541 Ma (Tables 1; S3). The modern ϵ_{Hf} values in these grains range from -1 to -
372 40 (Fig. 7, Table S3). There is no correlation between zircon crystallization age and
373 modern ϵ_{Hf} value (Fig. 7).

374

375 **6. DISCUSSION**

376 **6.1 Intrusion ages of western Newfoundland plutons**

377 For zircon from sample 1013002 of the Disappointment Hill Tonalite, removing
378 from further consideration analyses more than 10% normally discordant or 5% reverse
379 discordant leaves 30 analyses. The weighted mean $^{206}\text{Pb}/^{238}\text{U}$ age of these 30 analyses is
380 600 ± 8 Ma (MSWD = 0.7) including systematic errors (Fig. 8). We take this as the
381 intrusion age of the tonalite. This age overlaps within uncertainty the 606 ± 2 Ma intrusion
382 age published by Lin et al. (2013).

383 Zircon grain 13 in sample 1013005 of the Steel Mountain Anorthosite yielded a
384 $^{206}\text{Pb}/^{207}\text{Pb}$ age of 1141 ± 64 Ma, which is more than 500 M.y. older than the other ages from
385 this sample. We interpret this grain to be a xenocryst inherited from the Mesoproterozoic
386 rocks of the Corner Brook Lake block. Excluding the analysis of this xenocryst as well as
387 analyses more than 10% normally discordant or 5% reverse discordant leaves 11 analyses.
388 The weighted mean of these 11 analyses is 608 ± 12 Ma (MSWD=0.6) including systematic
389 errors (Fig. 8). We take this as the intrusion age of the anorthosite. The Ediacaran
390 intrusion age of the Steel Mountain Anorthosite is considerably younger than the
391 Mesoproterozoic intrusion age assumed in the absence of radiometric dating (Lin et al.,
392 2013). Based on our new dating, we now recognize that intrusion of the anorthosite was

Martin and Bosbyshell, 2018, Central Appalachian Exotic Terranes

393 broadly coeval with ca. 600 Ma intrusion of a granitic suite including the Disappointment
394 Hill Tonalite and the Round Pond Granite. Because of the similarity in intrusion ages, the
395 Steel Mountain Anorthosite perhaps should be considered part of the Corner Brook Lake
396 block, as is this granitic suite.

397 Analysis of spot 42 in sample 1013006 of the Round Pond Granite was 4.5%
398 reverse discordant and its $^{206}\text{Pb}/^{238}\text{U}$ age of 657 Ma is about 50 M.y. older than the
399 $^{206}\text{Pb}/^{238}\text{U}$ age of the next oldest concordant analysis. We interpret this grain to be a
400 xenocryst and do not use it for calculating the intrusion age of the granite. The $^{206}\text{Pb}/^{238}\text{U}$
401 age from spot 31 of 479 Ma is about 90 M.y. younger than the next youngest concordant
402 analysis. Crystals 12, 30, and 11 have $^{206}\text{Pb}/^{238}\text{U}$ ages of ca. 440, 555, and 557 Ma and
403 corresponding $^{206}\text{Pb}/^{207}\text{Pb}$ ages of 801, 713, and 739 Ma, respectively, and thus we
404 recognize these grains as xenocrysts. Based on the results from grains 12, 30, and 11, we
405 suggest grain 31 also is a xenocryst and do not use it in the calculation of the intrusion age.
406 Excluding spots 42 and 31 as well as analyses more than 10% normally discordant or 5%
407 reverse discordant leaves 21 analyses. The weighted mean of these 21 analyses is 590 ± 9
408 Ma (MSWD=0.8) including systematic errors (Fig. 8). We take this as the intrusion age of
409 the granite. Although this age overlaps with the multi-crystal thermal ionization mass
410 spectrometer (TIMS) age of 602 ± 10 Ma published by Williams et al. (1985) because of the
411 large uncertainties on both ages, the central value of the TIMS age is 12 M.y. older than the
412 central value of our laser ablation spot age. We now identify inherited zircon in this
413 sample, leading us to suggest that the TIMS age may be slightly too old because Williams
414 et al. (1985) did not recognize that some parts of the grains they analyzed were xenocrysts.

415

416 **6.2 Sources of magma to western Newfoundland plutons**

417 The main goal of this paper is not to elucidate the sources of melt for the Ediacaran
418 western Newfoundland plutons. Nevertheless, the zircon spot U-Pb and Lu-Hf isotope data
419 allow us to recognize that none of the three studied plutons was derived solely from the
420 depleted mantle. This conclusion is based on two types of data. First, the presence of
421 xenocrystic zircon in samples 1013005 and 1013006 requires assimilation of preexisting
422 crust into the Steel Mountain Anorthosite and Round Pond Granite magmas. Second, the
423 ϵ_{Hf} values of zircon in all three plutons were -7.8 to -16.5 at 600 Ma whereas the depleted
424 mantle ϵ_{Hf} value at this time was approximately +13 (Martin et al., 2018). The much more
425 negative values of all the analyzed zircon in the western Newfoundland plutons rule out
426 magma derivation purely from the depleted mantle.

427

428 **6.3 Maximum possible depositional ages of central Appalachian Piedmont sandstone**

429 In sample 314002 of the Storck quartzite, the two youngest analyses came from
430 grain 238 (499±44 Ma) and grain 76 (513±28 Ma) (Table S4). The weighted mean of these
431 two analyses is 509±23 Ma, which gives a maximum possible depositional age of 540 Ma.
432 If instead we reject grain 238 as too young and use the ages from grain 76 and grain 299
433 (524±22 Ma), the weighted mean is 520±17, which again yields a maximum depositional
434 age of 540 Ma. Accordingly, we take 540 Ma as the maximum possible depositional age of
435 the Storck quartzite. Hughes et al. (2014) similarly found that the maximum depositional
436 age of their sample of the Storck quartzite (their sample KSH-11-40) was Cambrian.

437 In sample 1213002 of the Hoods Mill rocks, grains 151 and 307 yielded the two
438 youngest $^{206}\text{Pb}/^{238}\text{U}$ ages, 521±40 and 529±22 Ma, respectively (Table S4). The weighted
439 mean of these ages is 528±19 Ma, which gives a maximum depositional age of 550 Ma.
440 Adding grains 92 (531±30 Ma) and 144 (531±30 Ma), the weighted mean of the four

Martin and Bosbyshell, 2018, Central Appalachian Exotic Terranes

441 youngest analyses is 529 ± 14 Ma, which likewise gives a maximum depositional age of 550
442 Ma. We thus take 550 Ma as the maximum depositional age of the Hoods Mill rocks based
443 on this sample. The youngest detrital zircon in the Hoods Mill rocks sample studied by
444 Martin et al. (2015) (their sample 1010002) had similar ages and the maximum depositional
445 age determined from their sample was comparable at 540 Ma.

446 Interpretation of the zircon ages in sample 1213003 of the Loch Raven Schist is
447 complicated by post-depositional growth of metamorphic zircon as well as lead loss from
448 detrital grains. Grains 253 through 165 yielded the youngest $^{206}\text{Pb}/^{238}\text{U}$ ages from this
449 sample and most of these crystals had U/Th ratios between 380 and 102 (Table S4).
450 Because of their youth and high U/Th ratios (see Hoskin and Schaltegger, 2003), we
451 interpret these 17 grains to have crystallized during metamorphism after deposition;
452 therefore we do not use these grains for determining maximum depositional age or
453 provenance. Grains 232 through 288 are older and had lower U/Th ratios than these 17
454 metamorphic crystals (Table S4). However, most of these grains were only 86-91%
455 concordant, and grain 324 was 4% reverse discordant with an age uncertainty of 100 M.y.
456 It is possible that these 8 grains are detrital grains that actually crystallized between ca. 488
457 and 459 Ma. However, the discordance of the analyses suggests that these could be detrital
458 grains with older crystallization ages. We conservatively choose not to use these 8 grains
459 for determination of the maximum depositional age or provenance in order to avoid
460 erroneously young ages. The next two youngest analyses came from grain 203 (507 ± 22
461 Ma; 97% concordant) and grain 213 (510 ± 44 Ma; 96% concordant). The weighted mean of
462 these two ages is 507 ± 20 Ma, which gives a maximum depositional age of 530 Ma.
463 Adding spot 310 (526 ± 24 Ma), the weighted mean of these three analyses is 515 ± 15 Ma,

Martin and Bosbyshell, 2018, Central Appalachian Exotic Terranes

464 which likewise gives a maximum depositional age of 530 Ma. We therefore take 530 Ma
465 as the maximum depositional age of the Loch Raven Schist.

466 With a $^{206}\text{Pb}/^{238}\text{U}$ age of 514 ± 28 Ma, grain 180 produced the youngest analysis
467 from sample 114002 of the Piney Run Formation (Table S4). However, no other ages from
468 this sample overlap the age of grain 180 within uncertainty, so we do not use the age of
469 grain 180 to determine the maximum depositional age of this formation. Grain 185
470 (1033 ± 46 Ma), grain 228 (1036 ± 38 Ma), and grain 148 (1037 ± 52 Ma) are the next three
471 youngest grains in sample 114002. The weighted mean of their ages is 1035 ± 25 Ma, which
472 gives a maximum depositional age of 1060 Ma for the Piney Run Formation.

473 Sample 114003 of the Pleasant Grove Schist produced two young grains with
474 $^{206}\text{Pb}/^{238}\text{U}$ ages that do not overlap with any other analyses within uncertainty: grain 10 at
475 519 ± 32 Ma and grain 309 at 629 ± 24 Ma (Table S4). The four youngest grains with ages
476 that do overlap within uncertainty are grain 165 (955 ± 132 Ma), grain 187 (969 ± 100 Ma),
477 grain 206 (988 ± 62 Ma) and grain 186 (989 ± 146 Ma). The weighted mean of these four
478 ages is 980 ± 46 Ma, which results in a maximum depositional age of 1030 Ma.

479 The ages of the two youngest grains in sample 314001 of the Prettyboy Schist, grain
480 124 (536 ± 22 Ma) and grain 240 (561 ± 28 Ma) overlap within uncertainty. The weighted
481 mean of these two ages is 546 ± 17 Ma. We therefore use 570 Ma as the maximum
482 depositional age of the Prettyboy Schist.

483 Interpretation of the ages of the zircon extracted from sample 314003 of the
484 sedimentary xenolith in the Brandywine Blue Gneiss is complicated by the presence of
485 metamorphic zircon (see also Aleinikoff et al., 2006). The youngest 37 zircon crystals,
486 from grain 45 to grain 183, have $^{206}\text{Pb}/^{238}\text{U}$ ages that overlap the intrusion age of the
487 Brandywine Blue Gneiss protolith (476 ± 6 Ma; Aleinikoff et al., 2006), considering

Martin and Bosbyshell, 2018, Central Appalachian Exotic Terranes

488 uncertainties (Table S4). We conservatively choose not to use these 37 ages for
489 interpretation of maximum depositional age or provenance in order to avoid inclusion of
490 grains with an age that is incorrectly too young. The two youngest grains with $^{206}\text{Pb}/^{238}\text{U}$
491 ages that do not overlap the gneiss protolith intrusion age within uncertainty are grain 242
492 (515 ± 24 Ma) and grain 162 (515 ± 34 Ma). The weighted mean of these two ages is 515 ± 19
493 Ma, which produces a maximum depositional age of 540 Ma. Adding the next youngest
494 analysis, 517 ± 24 Ma from grain 50, the weighted mean of the three ages becomes 516 ± 15
495 Ma, for a maximum depositional age of 540 Ma. We thus take 540 Ma as the maximum
496 depositional age of the sedimentary xenolith in the Brandywine Blue Gneiss.

497 The two youngest analyses from sample 114005 of the Wissahickon Formation
498 produced $^{206}\text{Pb}/^{238}\text{U}$ ages of 537 ± 48 Ma (grain 114) and 542 ± 34 (spot 23) (Table S4). The
499 weighted mean of these ages is 540 ± 28 Ma. The maximum depositional age of the
500 Wissahickon Formation therefore is 570 Ma.

501

502 **6.4 Central Appalachian Piedmont sandstone sediment provenance**

503 The tallest age peak in samples 114002, 114003, and 114005 of the Piney Run
504 Formation, Pleasant Grove Schist, and Wissahickon Formation lies at ca. 1460-1380 Ma
505 (Fig. S3). Each sample also has a major peak at ca. 1200-1170 Ma, a smaller Neoproterozoic
506 peak, a continuum of ages between ca. 1800 and 950 Ma, and one or two grains between
507 550 and 500 Ma. The results from sample 314001 of the Prettyboy Schist are similar, with
508 a main age peak at ca. 1050 Ma, one analysis at ca. 2500 Ma, a continuum of ages between
509 ca. 1500 and 950 Ma, and two analyses between ca. 560 and 530 Ma (Fig. S3). The
510 Mesoproterozoic main age peak in all four samples also is present in late Ediacaran-
511 Cambrian quartzite from the Blue Ridge Province directly to the west (Fig. 9; Satkoski,

Martin and Bosbyshell, 2018, Central Appalachian Exotic Terranes

512 2013). The source of the Blue Ridge sediment was Ediacaran Laurentia (Satkoski, 2013;
513 Smoot and Southworth, 2014). The spectrum of detrital zircon ages from the four new
514 samples also is similar to the age spectrum from many other Ediacaran-Cambrian quartzite
515 samples from the Piedmont Province of the central part of the Appalachian Orogen (Fig. 9).
516 Hughes et al. (2014) and Martin et al. (2015) showed that the sources of the zircon to these
517 Piedmont meta-sandstone samples could have been rocks in Ediacaran Laurentia. The
518 abundant ca. 1550-950 Ma grains could have come from the Granite-Rhyolite and
519 Grenville provinces directly west of the Appalachian Piedmont Province, whereas most of
520 the grains with other ages may have originated farther west (Whitmeyer and Karlstrom,
521 2007; Martin et al., 2015). This analysis holds for our four new samples as well. Because
522 of the viable sources in Ediacaran Laurentia and the similarity of the new ages to those
523 from the Blue Ridge Province, we interpret Ediacaran Laurentia as the source of sediment
524 to the type localities of the Piney Run Formation, Pleasant Grove Schist, Prettyboy Schist,
525 and Wissahickon Formation.

526 One motive for analyzing a new sample of the Storck quartzite and the Hoods Mill
527 rocks is to verify the detrital zircon age spectra reported by Hughes et al. (2014) and Martin
528 et al. (2015). Figure 10 confirms that the detrital zircon age spectrum from each of our new
529 samples is nearly identical to the previously reported age spectrum from each unit. Figure
530 10 also highlights the similarities in ages of detrital zircon from the Storck quartzite and the
531 Hoods Mill rocks. In both units, the main age peak is at ca. 630-600 Ma. Each unit
532 additionally contains zircon with ages both younger and older than this spike, with no large
533 gaps between ca. 2200 and 530 Ma.

534 Hughes et al. (2014) and Martin et al. (2015) concluded that Ediacaran Laurentia
535 was an unlikely source for the detrital zircon in the Storck quartzite and Hoods Mill rocks,

Martin and Bosbyshell, 2018, Central Appalachian Exotic Terranes

536 respectively, for two reasons. First, the main detrital zircon age peak in these samples is at
537 ca. 630-610 Ma, but Ediacaran Laurentia contained few felsic rocks with crystallization
538 ages between ca. 670 and 580 Ma (Whitmeyer and Karlstrom, 2007). Second, the ages of
539 detrital zircon from the Storck quartzite and Hoods Mill rocks do not form a prominent
540 Mesoproterozoic peak, but a major Mesoproterozoic age peak is a key signature of detrital
541 zircon derived from Ediacaran Laurentia. Hughes et al. (2014) and Martin et al. (2015)
542 instead proposed that Gondwana was the most likely source of the sediment to these units.
543 Figure 9 emphasizes that the ages of detrital zircon from the Storck quartzite and Hoods
544 Mill rocks are similar to detrital zircon ages from known peri-Gondwanan terranes but are
545 dissimilar to detrital zircon ages from sediment derived from Ediacaran Laurentia, such as
546 the late Ediacaran-Cambrian sandstone of the central Blue Ridge Province. Based on the
547 detrital zircon ages, we concur with the previous interpretations: Gondwana is a plausible
548 source of the sediment to the Storck quartzite and Hoods Mill rocks but Ediacaran
549 Laurentia is not.

550 To test whether the Neoproterozoic plutons in the Goochland Terrane or western
551 Newfoundland could have provided detrital zircon to the Storck quartzite or Hoods Mill
552 rocks, we compare the modern ϵ_{Hf} values of spots in zircon in Neoproterozoic plutons
553 from each area to the modern ϵ_{Hf} values of spots in the detrital zircon in samples 314002
554 and 1213002 that overlap the age range 670-580 Ma within uncertainty (Fig. 11). Most of
555 the ϵ_{Hf} values of the detrital zircon overlap the ϵ_{Hf} values of the zircon from the plutons.
556 However, one detrital grain from the Hoods Mill rocks has an ϵ_{Hf} value less negative than
557 the pluton zircon and three grains from the Hoods Mill rocks and one grain from the Storck
558 quartzite have an ϵ_{Hf} value more negative than the pluton zircon, outside uncertainty. It is
559 impossible to rule out the Goochland Terrane or western Newfoundland as sources of the

Martin and Bosbyshell, 2018, Central Appalachian Exotic Terranes

560 detrital zircon based on ϵ_{Hf} values because it is possible that a magmatic rock bearing
561 zircon with the appropriate Lu-Hf isotopic composition existed at the time of deposition of
562 the Storck quartzite or Hoods Mill rocks but that magmatic rock has since been eroded
563 away, leaving it unavailable for sampling. Nevertheless, the presence of detrital zircon
564 with modern ϵ_{Hf} values both less and more negative than any of the values measured in
565 zircon from the Neoproterozoic plutons is consistent with the derivation of Storck and
566 Hoods Mill sediment from a source other than the Goochland Terrane or western
567 Newfoundland. Moreover, the present-day ϵ_{Hf} values of the detrital zircon in the Storck
568 quartzite and Hoods Mill rocks mostly overlap the modern ϵ_{Hf} values of ca. 670-580 Ma
569 detrital zircon from a Ganderian sandstone, which range from -7 to -30 (Willner et al.,
570 2014).

571 Neither the U/Pb ages nor the present-day ϵ_{Hf} values of detrital zircon in the Storck
572 quartzite and Hoods Mill rocks are consistent with sediment derivation from Ediacaran
573 Laurentia. Further, the U/Pb ages of detrital zircon from these units are similar to the ages
574 of detrital zircon from late Ediacaran-Cambrian sandstone in known peri-Gondwanan
575 terranes. We therefore conclude that Gondwana was the most likely source of sediment to
576 the Storck quartzite and the Hoods Mill rocks. The Storck quartzite lies directly west of the
577 Chopawamsic Fault in northern Virginia and the Hoods Mill rocks crop out directly west of
578 the Plimmers Island Fault in northern Maryland (Fig. 2). Based on the occurrence of these
579 exotic rocks directly west of these two faults, we speculate that the faults might be
580 correlative.

581 In contrast to the other samples, interpretation of the provenance of the Loch Raven
582 Schist (sample 1213003) and the sedimentary xenolith in the Brandywine Blue Gneiss
583 (sample 314003) is not clear-cut. These units have late Mesoproterozoic to earliest

Martin and Bosbyshell, 2018, Central Appalachian Exotic Terranes

584 Neoproterozoic major age peaks, broadly similar to sediment derived from Ediacaran
585 Laurentia (Fig. 9). However, both samples also contain multiple detrital grains with U/Pb
586 ages between 670 and 580 Ma (Fig. S3; Table S4). The quantities of grains of this age are
587 intermediate between the numbers of such grains in the Storck quartzite and Hoods Mill
588 rocks and the quantities in samples with sediment derived from Ediacaran Laurentia. 24%
589 and 37% of the detrital zircon in the Storck quartzite and the Hoods Mill rocks,
590 respectively, have ages that overlap the range 670 to 580 Ma including uncertainties. These
591 proportions are 6% and 5% in the Loch Raven Schist and the sedimentary xenolith,
592 respectively, but fall to 1% and 0.4% in most central Piedmont quartzite of the same age
593 and central Blue Ridge late Ediacaran-Cambrian quartzite, respectively. Many central
594 Piedmont samples contain zero 670-580 Ma grains. Excluding the Storck quartzite, Hoods
595 Mill rocks, Loch Raven Schist, and the sedimentary xenolith, the central Piedmont sample
596 with the most grains in this age range is sample 909001 of the northern Sykesville
597 Formation, with 3% (Martin et al., 2015).

598 There are two plausible interpretations of the provenance of the detrital zircon in the
599 Loch Raven Schist and the sedimentary xenolith. One possibility is sediment derivation
600 from Ediacaran Laurentia. In this scenario, the ca. 670-580 Ma grains came from the
601 Goochland Terrane, western Newfoundland, or an unrecognized source in Ediacaran
602 Laurentia. The second option is sediment derivation from Gondwana. In this scenario, the
603 Loch Raven Schist and the sedimentary xenolith received more ca. 1200-900 Ma zircon
604 than is present in most other Gondwana-derived late Ediacaran-Cambrian sandstone due to
605 normal variations in the proportions of sediment transported by separate networks that
606 crossed large areas of a continent.

Martin and Bosbyshell, 2018, Central Appalachian Exotic Terranes

607 A challenge to option 1 is that no other units unequivocally derived from Ediacaran
608 Laurentia have so many ca. 670-580 Ma detrital grains. Sykesville Formation sample
609 909001 contains 3% detrital zircon of this age (Martin et al., 2015), but this remains a
610 lower percentage than in the Loch Raven Schist or the sedimentary xenolith. Further, the
611 Laurentian provenance of the Sykesville Formation is not unimpeachable. One point in
612 favor of option 2 is that there are examples of Gondwanan late Ediacaran-Cambrian
613 sandstone with age spectra similar to those in the Loch Raven Schist and the sedimentary
614 xenolith. For example, the Puncoviscana Formation in northwestern Argentina contains
615 many detrital grains with ages between ca. 1200-900 Ma (Fig. 9), including sample PMXX-
616 2 in Adams et al. (2011), which has a prominent ca. 1200 Ma age spike and no zircon
617 younger than 900 Ma. Schwartz and Gromet (2004) likewise found a metamorphosed
618 equivalent of the Puncoviscana Formation with a major age peak at ca. 1000 Ma; this peak
619 is larger than the ca. 600 Ma peak in this unit. Option 2 also has the advantage that other
620 units geographically near and geologically related to the Wilmington Complex contain
621 Gondwana-derived zircon. These units include the Chester Park Gneiss and rocks labeled
622 as the Wissahickon Formation (Bosbyshell et al., 2015). The latter unit is intercalated with
623 rocks of the Wilmington Complex. Based on the problem with option 1 and the merits of
624 option 2, we tentatively conclude that option 2 is the best interpretation. That is, the Loch
625 Raven Schist and the sedimentary xenolith might contain Gondwana-derived zircon, but
626 this conclusion is less certain for these units than for the Storck quartzite and the Hoods
627 Mill rocks. If the sedimentary xenolith in the Brandywine Blue Gneiss does contain
628 Gondwanan zircon, the Wilmington Complex island arc intruded sedimentary rocks that
629 were derived from Gondwana.

630

Martin and Bosbyshell, 2018, Central Appalachian Exotic Terranes

631 7. CONCLUSIONS

632 Our new U-Pb and Lu-Hf isotope data from spots in zircon support the following
633 conclusions.

- 634 1. Intrusion of the Steel Mountain Anorthosite, Disappointment Hill Tonalite, and
635 Round Pond Granite in western Newfoundland occurred at 608 ± 12 , 600 ± 8 , and
636 590 ± 9 Ma, respectively. Intrusion of the Steel Mountain Anorthosite is now
637 recognized to have been broadly coeval with intrusion of a granitic suite in western
638 Newfoundland at ca. 630-590.
- 639 2. The source of magma to the Steel Mountain Anorthosite, Disappointment Hill
640 Tonalite, and Round Pond Granite was not solely depleted mantle.
- 641 3. The maximum depositional age for most of our central Appalachian Piedmont
642 Province quartzite samples is late Ediacaran or Early Cambrian.
- 643 4. Sediment in our samples from the type localities of the Piney Run Formation,
644 Pleasant Grove Schist, Prettyboy Schist, and Wissahickon Formation was derived
645 from Ediacaran Laurentia.
- 646 5. Sediment in the Storck quartzite and the Hoods Mill rocks was derived from
647 Gondwana. We confirm the presence of a ca. 630-610 Ma peak in detrital zircon
648 ages in these units. The large proportions of detrital grains with ages between 670
649 and 580 Ma in these units is not consistent with derivation from Ediacaran
650 Laurentia but is similar to the age spectra of detrital zircon in much late Ediacaran-
651 Cambrian sandstone with a Gondwanan provenance. Modern ϵ_{Hf} values of some of
652 the 670-580 Ma detrital zircon likewise are inconsistent with derivation from the
653 scarce Neoproterozoic plutons in Ediacaran Laurentia.

Martin and Bosbyshell, 2018, Central Appalachian Exotic Terranes

654 6. The provenance of the sediment in the Loch Raven Schist and a sedimentary
655 xenolith in the Brandywine Blue Gneiss is less certain. However, these units
656 contain more ca. 670-580 Ma detrital zircon than any late Ediacaran-Cambrian
657 sandstone unequivocally derived from Ediacaran Laurentia, so we tentatively
658 conclude that Gondwana was the source of zircon to these units. If correct, this
659 conclusion means that the Brandywine Blue Gneiss, which is part of the
660 Wilmington Complex island arc, intruded sedimentary rocks derived from
661 Gondwana.

662

663 **ACKNOWLEDGEMENTS**

664 NSF grant EAR 1348685 to Martin supported this work. Philip Piccoli enabled our
665 use of the electron microprobe at the University of Maryland. We acknowledge the support
666 of the Maryland NanoCenter and its NispLab (Nanoscale Imaging, Spectroscopy, and
667 Properties Laboratory), which is supported in part by the National Science Foundation
668 (NSF) as a MRSEC (Materials Research Science and Engineering Center) shared
669 experimental facility. We are grateful to George Gehrels, Mark Pecha, and the staff of the
670 Arizona LaserChron Center for facilitating our zircon analyses in their laboratory. The
671 Arizona LaserChron Center is supported by NSF grant EAR 1338583. Michael C. Schmidt
672 provided invaluable field support in western Newfoundland. Elizabeth Pesar, Michael
673 Ream, and Todd Reitz contributed able laboratory assistance. **Reviewers and editor**

674

Martin and Bosbyshell, 2018, Central Appalachian Exotic Terranes

675 **REFERENCES**

- 676 Adams, C.J., Miller, H., Acenolaza, F.G., Toselli, A.J., and Griffin, W.L., 2011, The
677 Pacific Gondwana margin in the late Neoproterozoic–early Paleozoic: Detrital
678 zircon U–Pb ages from metasediments in northwest Argentina reveal their
679 maximum age, provenance and tectonic setting: *Gondwana Research*, v. 19, p. 71–
680 83, doi: 10.1016/j.gr.2010.05.002.
- 681 Aleinikoff, J.N., Horton, J.W., Jr., Drake, A.A., Jr., and Fanning, C.M., 2002, SHRIMP and
682 conventional U-Pb ages of Ordovician granites and tonalites in the central
683 Appalachian Piedmont: Implications for Paleozoic tectonic events: *American
684 Journal of Science*, v. 302, p. 50–75, doi: 10.2475/ajs.302.1.50.
- 685 Aleinikoff, J.N., Schenck, W.S., Plank, M.O., Srogi, L., Fanning, C.M., Kamo, S.L., and
686 Bosbyshell, H., 2006, Deciphering igneous and metamorphic events in high-grade
687 rocks of the Wilmington Complex, Delaware: Morphology, cathodoluminescence
688 and backscattered electron zoning, and SHRIMP U-Pb geochronology of zircon and
689 monazite: *Geological Society of America Bulletin*, v. 118, p. 39–64, doi:
690 10.1130/B25659.1.
- 691 Bailey, C., Eriksson, K.A., Allen, C.M., and Campbell, I.H., 2008, Detrital zircon
692 geochronology of the Chopawamsic Terrane, Virginia Piedmont: Evidence for a
693 non-Laurentian provenance, *in* Abstracts with Programs, Geological Society of
694 America, v. 40, p. 449.
- 695 Bascom, F., 1905, Piedmont district of Pennsylvania: *Geological Society of America
696 Bulletin*, v. 16, p. 289–328, doi: 10.1130/GSAB-16-289.
- 697 Bascom, F., 1902, The geology of the crystalline rocks of Cecil County, *in* Cecil County,
698 Baltimore, Maryland Geological Survey, p. 83–148.
- 699 van Berkel, J.T., and Currie, K.L., 1988, Geology of the Puddle Pond (12A/5) and Little
700 Grand Lake (12A/12) map areas, southwestern Newfoundland, *in* Current Research,
701 St. John's, Newfoundland Department of Mines, Mineral Development Division, v.
702 88–1, p. 99–107.
- 703 Bosbyshell, H., Crawford, M.L., and Srogi, L., 1999, Distribution of overprinting
704 metamorphic mineral assemblages in the Wissahickon group, southeastern
705 Pennsylvania, *in* Valentino, D.W. and Gates, A.E. eds., *The Mid-Atlantic Piedmont:
706 Tectonic Missing Link of the Appalachians*, Boulder, Geological Society of
707 America, Special Paper, v. 330, p. 41–58, doi: 10.1130/0-8137-2330-2.41.
- 708 Bosbyshell, H., Srogi, L., and Blackmer, G.C., 2016, Monazite age constraints on the
709 tectono-thermal evolution of the central Appalachian Piedmont: *American
710 Mineralogist*, v. 101, p. 1820–1838, doi: 10.2138/am-2016-5482.
- 711 Bosbyshell, H., Srogi, L., Blackmer, G.C., Schenck, W.S., Mathur, R., and Valencia, V.,
712 2015, The tectono-thermal evolution of the central Appalachian Orogen: Accretion
713 of a peri-Gondwanan(?) Ordovician arc, *in* Brezinski, D.K., Halka, J.P., and Ortt,
714 R.A., Jr. eds., *Tripping from the Fall Line: Field Excursions for the GSA Annual
715 Meeting, Baltimore, 2015*, Geological Society of America, Field Guide, v. 40, p.
716 35–59, doi: 10.1130/2015.0040(03).
- 717 Brem, A.G., Lin, S., and van Staal, C.R., 2006, Geology, Harrys River, Newfoundland and
718 Labrador: Geological Survey of Canada Open File 4921, scale 1:50,000, doi:
719 10.4095/223017.
- 720 Cawood, P.A., van Gool, J.A., and Dunning, G.R., 1995, Collisional tectonics along the
721 Laurentian margin of the Newfoundland Appalachians, *in* Hibbard, J.P., van Staal,

Martin and Bosbyshell, 2018, Central Appalachian Exotic Terranes

- 722 C.R., and Cawood, P.A. eds., Current Perspectives in the Appalachian-Caledonian
723 Orogen, Geological Association of Canada, Special Paper, v. 41, p. 283–301.
- 724 Cawood, P.A., van Gool, J.A.M., and Dunning, G.R., 1996, Geological development of
725 eastern Humber and western Dunnage zones: Corner Brook–Glover Island region,
726 Newfoundland: Canadian Journal of Earth Sciences, v. 33, p. 182–198, doi:
727 10.1139/e96-017.
- 728 Cawood, P.A., and Nemchin, A.A., 2001, Paleogeographic development of the east
729 Laurentian margin: Constraints from U–Pb dating of detrital zircons in the
730 Newfoundland Appalachians: Geological Society of America Bulletin, v. 113, p.
731 1234–1246, doi: 10.1130/0016-7606(2001)113<1234:PDOTEL>2.0.CO;2.
- 732 Crowley, W.P., 1976, The geology of the crystalline rocks near Baltimore and its bearing
733 on the evolution of the eastern Maryland Piedmont: Maryland Geological Survey
734 Report of Investigations RI 27, 40 p.
- 735 Currie, K.L., van Breeman, O., Hunt, P.A., and van Berkel, J.T., 1992, Age of high-grade
736 gneisses south of Grand Lake, Newfoundland: Atlantic Geology, v. 28, p. 153–161,
737 doi: 10.4138/1857.
- 738 Dickinson, W.R., and Gehrels, G.E., 2009, Use of U–Pb ages of detrital zircons to infer
739 maximum depositional ages of strata: A test against a Colorado Plateau Mesozoic
740 database: Earth and Planetary Science Letters, v. 288, p. 115–125, doi:
741 10.1016/j.epsl.2009.09.013.
- 742 Drake, A.A., 1989, Metamorphic rocks of the Potomac Terrane in the Potomac Valley of
743 Virginia and Maryland, *in* 28th International Geological Congress, Field trip
744 guidebook, Washington, D.C., American Geophysical Union, v. T202, p. 1–22, doi:
745 10.1029/FT202.
- 746 Farrar, S.S., 1984, The Goochland granulite terrane: Remobilized Grenville basement in the
747 eastern Virginia Piedmont, *in* Bartholomew, M.J. ed., The Grenville Event in the
748 Appalachians and Related Topics, Boulder, Geological Society of America, Special
749 Paper, v. 194, p. 215–228, doi: 10.1130/SPE194-p215.
- 750 Fisher, G.W., Higgins, M.W., and Zietz, I., 1979, Geological interpretations of
751 aeromagnetic maps of the crystalline rocks in the Appalachians, Northern Virginia
752 to New Jersey: Maryland Geological Survey Report of Investigations RI 32, 43 p.
- 753 Fisher, C.M., Vervoort, J.D., and DuFrane, S.A., 2014, Accurate Hf isotope determinations
754 of complex zircons using the “laser ablation split stream” method: Geochemistry,
755 Geophysics, Geosystems, v. 15, p. 121–139, doi: 10.1002/2013GC004962.
- 756 Gehrels, G., and Pecha, M., 2014, Detrital zircon U–Pb geochronology and Hf isotope
757 geochemistry of Paleozoic and Triassic passive margin strata of western North
758 America: Geosphere, v. 10, p. 49–65, doi: 10.1130/GES00889.1.
- 759 Gehrels, G.E., Valencia, V.A., and Ruiz, J., 2008, Enhanced precision, accuracy, efficiency,
760 and spatial resolution of U–Pb ages by laser ablation-multicollector-inductively
761 coupled plasma-mass spectrometry: Geochemistry, Geophysics, Geosystems, v. 9,
762 Q03017, doi: 10.1029/2007GC001805.
- 763 Glover, III, L., Sheridan, R.E., Holbrook, W.S., Ewing, J., Talwani, M., Hawman, R.B.,
764 and Wang, P., 1997, Paleozoic collisions, Mesozoic rifting, and structure of the
765 Middle Atlantic states continental margin: An “EDGE” Project report, *in* Glover,
766 III, L. and Gates, A.E. eds., Central and Southern Appalachian sutures: results of the
767 EDGE Project and related studies, Boulder, Geological Society of America, Special
768 Paper, v. 314, p. 107–135, doi: 10.1130/0-8137-2314-0.107.

Martin and Bosbyshell, 2018, Central Appalachian Exotic Terranes

- 769 Hatcher, R.D., Jr., 1989, Appalachians introduction, *in* Hatcher, R.D., Thomas, W.A., and
770 Viele, G.W. eds., *The Appalachian-Ouachita Orogen in the United States*, Boulder,
771 Geological Society of America, *Geology of North America*, v. F-2, p. 1–6, doi:
772 10.1130/DNAG-GNA-F2.1.
- 773 Hibbard, J.P., Miller, B.V., Hames, W.E., Standard, I.D., Allen, J.S., Lavallee, S.B., and
774 Boland, I.B., 2012, Kinematics, U-Pb geochronology, and $^{40}\text{Ar}/^{39}\text{Ar}$
775 thermochronology of the Gold Hill shear zone, North Carolina: The Cherokee
776 orogeny in Carolina, *Southern Appalachians: Geological Society of America*
777 *Bulletin*, v. 124, p. 643–656, doi: 10.1130/B30579.1.
- 778 Hibbard, J.P., van Staal, C.R., Rankin, D.W., and Williams, H., 2006, Lithotectonic map of
779 the Appalachian Orogen, Canada-United States of America: Geological Survey of
780 Canada, Map 2096A, 1:1,500,000, doi: 10.4095/221912.
- 781 Higgins, M.W., 1972, Age, origin, regional relations, and nomenclature of the Glenarm
782 Series, central Appalachian Piedmont: A reinterpretation: *Geological Society of*
783 *America Bulletin*, v. 83, p. 989, doi: 10.1130/0016-
784 7606(1972)83[989:AORRAN]2.0.CO;2.
- 785 Hopson, C.A., 1964, The crystalline rocks of Howard and Montgomery counties, *in* *The*
786 *geology of Howard and Montgomery counties*, Baltimore, Maryland Geological
787 Survey, p. 27–215.
- 788 Horton, J.W., Jr., Aleinikoff, J.N., Drake, A.A., Jr., and Fanning, C.M., 2010, Ordovician
789 volcanic-arc terrane in the Central Appalachian Piedmont of Maryland and Virginia:
790 SHRIMP U-Pb geochronology, field relations, and tectonic significance, *in* Tollo,
791 R.P., Bartholomew, M.J., Hibbard, J.P., and Karabinos, P.M. eds., *From Rodinia to*
792 *Pangea: The Lithotectonic Record of the Appalachian Region*, Boulder, Geological
793 Society of America, *Memoir*, v. 206, p. 621–660, doi: 10.1130/2010.1206(25).
- 794 Horton, J.W., Jr., Drake, A.A., Jr., and Rankin, D.W., 1989, Tectonostratigraphic terranes
795 and their Paleozoic boundaries in the central and southern Appalachians, *in*
796 Dallmeyer, R.D. ed., *Terranes in the Circum-Atlantic Paleozoic Orogens*, Boulder,
797 Geological Society of America, *Special Paper*, v. 230, p. 213–246, doi:
798 10.1130/SPE230-p213.
- 799 Hoskin, P.W.O., and Schaltegger, U., 2003, The composition of zircon and igneous and
800 metamorphic petrogenesis: *Reviews in Mineralogy and Geochemistry*, v. 53, p. 27–
801 62, doi: 10.2113/0530027.
- 802 Hughes, K.S., Hibbard, J.P., and Miller, B.V., 2013, Relationship between the Ellisville
803 pluton and Chopawamsic fault: Establishment of significant Late Ordovician
804 faulting in the Appalachian Piedmont of Virginia: *American Journal of Science*, v.
805 313, p. 584–612, doi: 10.2475/06.2013.03.
- 806 Hughes, K.S., Hibbard, J.P., Pollock, J.C., Lewis, D.J., and Miller, B.V., 2014, Detrital
807 zircon geochronology across the Chopawamsic Fault, western Piedmont of North-
808 Central Virginia: Implications for the main Iapetan suture in the southern
809 Appalachian Orogen: *Geoscience Canada*, v. 41, p. 503–522, doi:
810 10.12789/geocanj.2014.41.052.
- 811 Ibanez-Mejia, M., Pullen, A., Arenstein, J., Gehrels, G.E., Valley, J., Ducea, M.N., Mora,
812 A.R., Pecha, M., and Ruiz, J., 2015, Unraveling crustal growth and reworking
813 processes in complex zircons from orogenic lower-crust: The Proterozoic Putumayo
814 Orogen of Amazonia: *Precambrian Research*, v. 267, p. 285–310, doi:
815 10.1016/j.precamres.2015.06.014.

Martin and Bosbyshell, 2018, Central Appalachian Exotic Terranes

- 816 Jonas, A.I., and Stose, G.W., 1938, New formation names used on the geologic map of
817 Frederick County, Maryland: *Journal of the Washington Academy of Sciences*, v.
818 28, p. 345–348.
- 819 Kemp, A.I.S., Hawkesworth, C.J., Paterson, B.A., and Kinny, P.D., 2006, Episodic growth
820 of the Gondwana supercontinent from hafnium and oxygen isotopes in zircon:
821 *Nature*, v. 439, p. 580–583, doi: 10.1038/nature04505.
- 822 Knopf, E.B., and Jonas, A.I., 1923, Stratigraphy of the crystalline schists of Pennsylvania
823 and Maryland: *American Journal of Science*, v. s5-5, p. 40–62, doi: 10.2475/ajs.s5-
824 5.25.40.
- 825 Kunk, M.J., Wintsch, R.P., Naeser, C.W., Naeser, N.D., Southworth, C.S., Drake, A.A.,
826 and Becker, J.L., 2005, Contrasting tectonothermal domains and faulting in the
827 Potomac terrane, Virginia–Maryland—discrimination by $^{40}\text{Ar}/^{39}\text{Ar}$ and fission-
828 track thermochronology: *Geological Society of America Bulletin*, v. 117, p. 1347–
829 1366, doi: 10.1130/B25599.1.
- 830 Li, Z.X., Bogdanova, S.V., Collins, A.S., Davidson, A., De Waele, B., Ernst, R.E.,
831 Fitzsimons, I.C.W., Fuck, R.A., Gladkochub, D.P., Jacobs, J., Karlstrom, K.E., Lu,
832 S., Natapov, L.M., Pease, V., et al., 2008, Assembly, configuration, and break-up
833 history of Rodinia: A synthesis: *Precambrian Research*, v. 160, p. 179–210, doi:
834 10.1016/j.precamres.2007.04.021.
- 835 Lin, S., Brem, A.G., van Staal, C.R., Davis, D.W., McNicoll, V.J., and Pehrsson, S., 2013,
836 The Corner Brook Lake block in the Newfoundland Appalachians: A suspect
837 terrane along the Laurentian margin and evidence for large-scale orogen-parallel
838 motion: *Geological Society of America Bulletin*, v. 125, p. 1618–1632, doi:
839 10.1130/B30805.1.
- 840 Ludwig, K.R., 2008, User’s manual for Isoplot 3.70: Berkeley Geochronology Center
841 Special Publication 4, 76 p.
- 842 Macdonald, F.A., Ryan-Davis, J., Coish, R.A., Crowley, J.L., and Karabinos, P., 2014, A
843 newly identified Gondwanan terrane in the northern Appalachian Mountains:
844 Implications for the Taconic orogeny and closure of the Iapetus Ocean: *Geology*, v.
845 42, p. 539–542, doi: 10.1130/G35659.1.
- 846 Martin, A.J., Southworth, S., Collins, J.C., Fisher, S.W., and Kingman, E.R.I., 2015,
847 Laurentian and Amazonian sediment sources to Neoproterozoic–lower Paleozoic
848 Maryland Piedmont rocks: *Geosphere*, v. 11, p. 1042–1061, doi:
849 10.1130/GES01140.1.
- 850 Mathews, E.B., 1905, Correlation of Maryland and Pennsylvania Piedmont formations:
851 *Geological Society of America Bulletin*, v. 16, p. 329–346, doi: 10.1130/GSAB-16-
852 329.
- 853 Mathews, E.B., 1904, The structure of the Piedmont Plateau as shown in Maryland:
854 *American Journal of Science*, v. s4-17, p. 141–159, doi: 10.2475/ajs.s4-17.98.141.
- 855 Mathews, E.B., and Grasty, J.S., 1909, The limestones of Maryland; with special reference
856 to their use in the manufacture of lime and cement, *in* Maryland Geological Survey,
857 Special Publication, v. 8, part 3, p. 227–486.
- 858 Mattinson, J.M., 2010, Analysis of the relative decay constants of ^{235}U and ^{238}U by
859 multi-step CA-TIMS measurements of closed-system natural zircon samples:
860 *Chemical Geology*, v. 275, p. 186–198, doi: 10.1016/j.chemgeo.2010.05.007.
- 861 Owens, B.E., Buchwaldt, R., and Shirvell, C.R., 2010, Geochemical and geochronological
862 evidence for Devonian magmatism revealed in the Maidens gneiss, Goochland

Martin and Bosbyshell, 2018, Central Appalachian Exotic Terranes

- 863 terrane, Virginia, *in* Tollo, R.P., Bartholomew, M.J., Hibbard, J.P., and Karabinos,
864 P.M. eds., *From Rodinia to Pangea: The Lithotectonic Record of the Appalachian*
865 *Region*, Boulder, Geological Society of America, Memoir, v. 206, p. 725–738, doi:
866 10.1130/2010.1206(28).
- 867 Owens, B.E., and Tucker, R.D., 2003, Geochronology of the Mesoproterozoic State Farm
868 gneiss and associated Neoproterozoic granitoids, Goochland terrane, Virginia:
869 Geological Society of America Bulletin, v. 115, p. 972–982, doi:
870 10.1130/B25258.1.
- 871 Plank, M.O., Schenck, W.S., and Srogi, L., 2000, Bedrock geology of the Piedmont of
872 Delaware and adjacent Pennsylvania: Delaware Geological Survey Report of
873 Investigations 59, 52 p.
- 874 Pollock, J.C., Hibbard, J.P., and van Staal, C.R., 2012, A paleogeographical review of the
875 peri-Gondwanan realm of the Appalachian orogen: *Canadian Journal of Earth*
876 *Sciences*, v. 49, p. 259–288, doi: 10.1139/e11-049.
- 877 Pollock, J.C., Hibbard, J.P., and Sylvester, P.J., 2010, Depositional and tectonic setting of
878 the Neoproterozoic–early Paleozoic rocks of the Virgilina sequence and Albemarle
879 Group, North Carolina, *in* Tollo, R.P., Bartholomew, M.J., Hibbard, J.P., and
880 Karabinos, P.M. eds., *From Rodinia to Pangea: The Lithotectonic Record of the*
881 *Appalachian Region*, Boulder, Geological Society of America, Memoir, v. 206, p.
882 739–772, doi: 10.1130/2010.1206(29).
- 883 Pullen, A., Ibanez-Mejia, M., Gehrels, G.E., Ibanez-Mejia, J.C., and Pecha, M., 2014, What
884 happens when n=1000? Creating large-n geochronological datasets with LA-ICP-
885 MS for geologic investigations: *Journal of Analytical Atomic Spectrometry*, v. 29,
886 p. 971–980, doi: 10.1039/c4ja00024b.
- 887 Reinhardt, J., 1977, Cambrian off-shelf sedimentation, central Appalachians, *in* Cook, H.E.
888 and Enos, P. eds., *Deep-water carbonate environments*, Society of Economic
889 Paleontologists and Mineralogists (SEPM), Special Publication, v. 25, p. 83–112.
- 890 Reinhardt, J., 1974, Stratigraphy, sedimentology and Cambro-Ordovician paleogeography
891 of the Frederick Valley, Maryland: Maryland Geological Survey Report of
892 Investigations RI 23, 74 p.
- 893 Rodgers, J., 1970, *The tectonics of the Appalachians*: New York, Wiley-Interscience, 271
894 p.
- 895 Satkoski, A., 2013, Sr-Nd-Hf isotope geochemistry of 3.5 Ga gneisses of the Minnesota
896 River Valley and U-Pb geochronology of detrital zircon from Cambrian
897 sedimentary rocks of the Laurentian rifted margin [Ph.D. Dissertation]: Syracuse
898 University, 215 p.
- 899 Scherer, E., Munker, C., and Mezger, K., 2001, Calibration of the lutetium-hafnium clock:
900 *Science*, v. 293, p. 683–687, doi: 10.1126/science.1061372.
- 901 Schwartz, J.J., and Gromet, L.P., 2004, Provenance of a late Proterozoic–early Cambrian
902 basin, Sierras de Cordoba, Argentina: *Precambrian Research*, v. 129, p. 1–21, doi:
903 10.1016/j.precamres.2003.08.011.
- 904 Scotese, C.R., and Langford, R.P., 1995, Pangea and the paleogeography of the Permian, *in*
905 Scholle, P.A., Peryt, T.M., and Ulmer-Scholle, D.S. eds., *The Permian of northern*
906 *Pangea*, Berlin, Springer, p. 3–19, doi: 10.1007/978-3-642-78593-1_1.
- 907 Slama, J., Kosler, J., Condon, D.J., Crowley, J.L., Gerdes, A., Hanchar, J.M., Horstwood,
908 M.S.A., Morris, G.A., Nasdala, L., Norberg, N., Schaltegger, U., Schoene, B.,
909 Tubrett, M.N., and Whitehouse, M.J., 2008, Plesovice zircon — A new natural

Martin and Bosbyshell, 2018, Central Appalachian Exotic Terranes

- 910 reference material for U–Pb and Hf isotopic microanalysis: *Chemical Geology*, v.
 911 249, p. 1–35, doi: 10.1016/j.chemgeo.2007.11.005.
- 912 Smoot, J.P., and Southworth, S., 2014, Volcanic rift margin model for the rift-to-drift
 913 setting of the late Neoproterozoic-early Cambrian eastern margin of Laurentia:
 914 Chilhowee Group of the Appalachian Blue Ridge: *Geological Society of America*
 915 *Bulletin*, v. 126, p. 201–218, doi: 10.1130/B30875.1.
- 916 Soderlund, U., Patchett, P.J., Vervoort, J.D., and Isachsen, C.E., 2004, The ^{176}Lu decay
 917 constant determined by Lu–Hf and U–Pb isotope systematics of Precambrian mafic
 918 intrusions: *Earth and Planetary Science Letters*, v. 219, p. 311–324, doi:
 919 10.1016/S0012-821X(04)00012-3.
- 920 Southwick, D.L., and Fisher, G.W., 1967, Revision of stratigraphic nomenclature of the
 921 Glenarm Series in Maryland: Maryland Geological Survey Report of Investigations
 922 RI 6, 19 p.
- 923 Southworth, S., Brezinski, D.K., Drake, A.A., Jr., Burton, W.C., Orndorff, R.C., Froelich,
 924 A.J., Reddy, J.E., Denenny, D., and Daniels, D.L., 2007, Geologic map of the
 925 Frederick 30' × 60' quadrangle, Maryland, Virginia, and West Virginia: United
 926 States Geological Survey Scientific Investigations Map 2889, scale 1:100,000, 42 p.
- 927 van Staal, C.R., Whalen, J.B., Valverde-Vaquero, P., Zagorevski, A., and Rogers, N., 2009,
 928 Pre-Carboniferous, episodic accretion-related, orogenesis along the Laurentian
 929 margin of the northern Appalachians, *in* Murphy, J.B., Keppie, J.D., and Hynes,
 930 A.J. eds., *Ancient Orogens and Modern Analogues*, London, Geological Society,
 931 Special Publication, v. 327, p. 271–316, doi:10.1144/SP327.13.
- 932 Stacey, J.S., and Kramers, J.D., 1975, Approximation of terrestrial lead isotope evolution
 933 by a two-stage model: *Earth and Planetary Science Letters*, v. 26, p. 207–221, doi:
 934 10.1016/0012-821X(75)90088-6.
- 935 Virginia Geological Survey, 1928, Geologic map of Virginia: Virginia Geological Survey,
 936 scale 1:500,000.
- 937 Whitmeyer, S.J., and Karlstrom, K.E., 2007, Tectonic model for the Proterozoic growth of
 938 North America: *Geosphere*, v. 3, p. 220–259, doi: 10.1130/GES00055.1.
- 939 Williams, G.H., 1892, Guide to Baltimore with an account of the geology of its environs;
 940 guidebook prepared by the local committee for the meeting of the American
 941 Institute of Mining Engineers: Baltimore, John Murphy and Company, 139 p.
- 942 Williams, G.H., 1891, The petrography and structure of the Piedmont Plateau in Maryland:
 943 *Geological Society of America Bulletin*, v. 2, p. 301–322, doi: 10.1130/GSAB-2-
 944 301.
- 945 Williams, H., Gillespie, R.T., and Van Breemen, O., 1985, A late Precambrian rift-related
 946 igneous suite in western Newfoundland: *Canadian Journal of Earth Sciences*, v. 22,
 947 p. 1727–1735, doi: 10.1139/e85-181.
- 948 Willner, A.P., Gerdes, A., Massonne, H.-J., Van Staal, C.R., and Zagorevski, A., 2014,
 949 Crustal evolution of the northeast Laurentian margin and the peri-Gondwanan
 950 microcontinent Ganderia prior to and during closure of the Iapetus Ocean: detrital
 951 zircon U–Pb and Hf isotope evidence from Newfoundland: *Geoscience Canada*, v.
 952 41, p. 345–364, doi: 10.12789/geocanj.2014.41.046.
- 953 Wintsch, R.P., Kunk, M.J., Mulvey, B.K., and Southworth, C.S., 2010, $^{40}\text{Ar}/^{39}\text{Ar}$ dating
 954 of Silurian and Late Devonian cleavages in lower greenschist-facies rocks in the
 955 Westminster terrane, Maryland, USA: *Geological Society of America Bulletin*, v.
 956 122, p. 658–677, doi: 10.1130/B30030.1.

Martin and Bosbyshell, 2018, Central Appalachian Exotic Terranes

- 957 Woodhead, J.D., and Hergt, J.M., 2005, A preliminary appraisal of seven natural zircon
958 reference materials for in situ Hf isotope determination: *Geostandards and*
959 *Geoanalytical Research*, v. 29, p. 183–195, doi: 10.1111/j.1751-
960 908X.2005.tb00891.x.
- 961 Woodhead, J., Hergt, J., Shelley, M., Eggins, S., and Kemp, R., 2004, Zircon Hf-isotope
962 analysis with an excimer laser, depth profiling, ablation of complex geometries, and
963 concomitant age estimation: *Chemical Geology*, v. 209, p. 121–135, doi:
964 10.1016/j.chemgeo.2004.04.026.

Draft

965 **FIGURE CAPTIONS**

- 966 1. Generalized geologic map of the Appalachian Orogen. Modified from Hibbard et al.
967 (2006).
- 968 2. Geologic map of part of the central Appalachian Piedmont Province. Modified from
969 Hibbard et al. (2006), Southworth et al. (2007), Hughes et al. (2014), and Martin et al.
970 (2015).
- 971 3. Geologic map of part of western Newfoundland. Modified from Brem et al. (2006) and
972 Lin et al. (2013).
- 973 4. Backscattered electron (left column) and cathodoluminescence (right column) images
974 of zircon from the three samples of western Newfoundland intrusive rocks. The circles
975 show the locations of 20 μm -diameter laser spots that yielded the indicated $^{206}\text{Pb}/^{238}\text{U}$
976 ages.
- 977 5. Concordia diagrams for U/Pb isotope analyses of spots in zircon from the three samples
978 of western Newfoundland intrusive rocks.
- 979 6. Modern ϵHf values of spots in zircon from the three samples of western Newfoundland
980 intrusive rocks.
- 981 7. Modern ϵHf values versus crystallization age for detrital zircon from the Storck
982 quartzite and the Hoods Mill rocks. There is no correlation between zircon
983 crystallization age and modern ϵHf value.
- 984 8. Plots of concordant, non-xenocrystic U-Pb isotope analyses (vertical red bars) from
985 each sample of western Newfoundland intrusive rocks showing the weighted mean
986 $^{206}\text{Pb}/^{238}\text{U}$ age (horizontal green bar). The reported uncertainty includes both
987 measurement and systematic errors.

Martin and Bosbyshell, 2018, Central Appalachian Exotic Terranes

- 988 9. Normalized relative probability plots of detrital zircon ages from our samples compared
989 to detrital zircon ages from other late Ediacaran-Cambrian Laurentian and peri-
990 Gondwanan sandstone. Data were normalized so that the area under each curve is the
991 same. Data sources and processing details are given in Table S5 and the ages and
992 corresponding errors are in Table S6. The sample numbers for the Piney Run
993 Formation, Pleasant Grove Schist, Prettyboy Schist, and Wissahickon Formation are
994 114002, 114003, 314001, and 114005, respectively.
- 995 10. Normalized relative probability plots of detrital zircon ages from the Storck quartzite
996 and the Hoods Mill rocks. The detrital zircon age spectra from our new samples are
997 nearly identical to the previously-published spectra from these units. Data were
998 normalized so that the area under each curve is the same. Data processing is described
999 in Table S5.
- 1000 11. Comparison of present-day ϵHf values of 670-580 Ma detrital zircon from the Storck
1001 quartzite and the Hoods Mill rocks with modern ϵHf values of zircon in Neoproterozoic
1002 plutons in the Goochland Terrane and western Newfoundland. The present-day ϵHf
1003 values of the detrital zircon extend to values both less and more negative than the zircon
1004 in the plutons, outside uncertainty. The plot shows only detrital grains with ages that
1005 overlap the age range 670-580 Ma within uncertainty. These are grains 131 to 218 in
1006 sample 314002 and 69 to 266 in sample 1213002 (Table S3). The range of ϵHf values
1007 for the zircon in the plutons includes uncertainties. The bands of values for the plutons
1008 are shown stretching horizontally across the entire diagram to ease viewing, but the
1009 actual range of intrusion ages is 630-590 and 660-580 Ma for the western
1010 Newfoundland and Goochland plutons, respectively. ϵHf values for the Goochland
1011 Terrane zircon from Martin et al. (2018).

1012

1013 **TABLES**

1014 1. Central Appalachian Piedmont meta-sandstone sample summary.

1015 2. Western Newfoundland igneous rocks sample summary.

1016

1017 **ELECTRONIC SUPPLEMENT**1018 **FIGURES**

1019 Figure S1: Photomicrographs of thin sections of each sample. The scale is the same for
1020 each image. In (B), all minerals in the field of view are plagioclase feldspar.

1021 Abbreviations: amp-amphibole, bt-biotite, chl-chlorite, fsp-feldspar, grt-garnet, ms-
1022 muscovite, q-quartz.

1023

1024 Figure S2: Measured $^{176}\text{Hf}/^{177}\text{Hf}$ ratios of spots in the seven zircon standards acquired
1025 throughout the Lu-Hf isotope analysis session. The horizontal green bar indicates the
1026 weighted mean.

1027

1028 Figure S3: Histograms and relative probability plots of the U/Pb isotopic ages of detrital
1029 zircon from each central Appalachian Piedmont meta-sandstone sample. Best age is the
1030 $^{206}\text{Pb}/^{238}\text{U}$ date for grains with a $^{206}\text{Pb}/^{207}\text{Pb}$ date younger than 900 Ma and $^{206}\text{Pb}/^{207}\text{Pb}$ date
1031 for older grains.

1032

1033 **TABLES**

1034 Table S1: Western Newfoundland igneous zircon spot U-Pb isotope data.

1035

Martin and Bosbyshell, 2018, Central Appalachian Exotic Terranes

1036 Table S2: Summary of U/Pb ages of standard zircon analyzed along with zircon from the
1037 samples.

1038

1039 Table S3: Zircon spot Lu-Hf isotope data.

1040

1041 Table S4: Central Appalachian Piedmont detrital zircon spot U-Pb isotope data.

1042

1043 Table S5: Data sources and processing details for Figure 9.

1044

1045 Table S6: Data used to make Figure 9.

Draft

TABLE 1. SUMMARY OF META-SANDSTONE SAMPLES FROM THE CENTRAL APPALACHIAN PIEDMONT

Sample number	Formation name	Informal name	Latitude °N	Longitude °W	Number of U/Pb analyses kept	Max depo age (Ma), this study	U/Pb ages of individual zircon analyses used to determine max depo age (Ma)	Number of Hf analyses	Reference
<i>Central Virginia</i>									
314002	Mine Run Complex I	Storck quartzite	38.41843	77.63513	269	540	499, 513	40	Hughes et al., 2014
<i>Northern Maryland</i>									
1213002	Mather Gorge	Hoods Mill rocks ^b	39.35212	77.01553	252	550	521, 529	22	Martin et al., 2015
1213003 ^a	Loch Raven Schist	-	39.50111	76.62347	169	530	507, 510	not analyzed	Crowley, 1976
114002 ^a	Piney Run	-	39.53998	76.77674	167	1060	1033, 1036, 1037	not analyzed	Crowley, 1976
114003 ^a	Pleasant Grove Schist	-	39.54285	76.80614	273	1030	955, 969, 988, 989	not analyzed	Crowley, 1976
314001 ^a	Prettyboy Schist	-	39.61900	76.70773	287	570	536, 561	not analyzed	Crowley, 1976
<i>Northern Delaware</i>									
314003	Brandywine Blue Gneiss	sedimentary xenolith ^b	39.77823	75.50748	208	540	515, 515	not analyzed	Plank et al., 2000
<i>Southeastern Pennsylvania</i>									
114005 ^a	Wissahickon	-	40.05671	75.21819	209	570	537, 542	not analyzed	Bascom, 1905
Totals:					1834	analyses from 8 samples		62	analyses from 2 samples

^aType locality.^bInformal name assigned in this study.

TABLE 2. SUMMARY OF WESTERN NEWFOUNDLAND IGNEOUS SAMPLES

Sample number	Unit name	Latitude °N	Longitude °W	Number of zircon Hf analyses	Igneous crystallization age (Ma)	Igneous crystallization age reference
1013002	Disappointment Hill Tonalite	48.58884	58.14222	15	606 ± 2	Lin et al., 2013
1013005	Steel Mountain Anorthosite	48.55948	58.15767	6	608 ± 12	this study
1013006	Round Pond Granite	49.06184	57.70439	9	590 ± 9	this study
Total:				30	analyses from 3 samples	

Draft

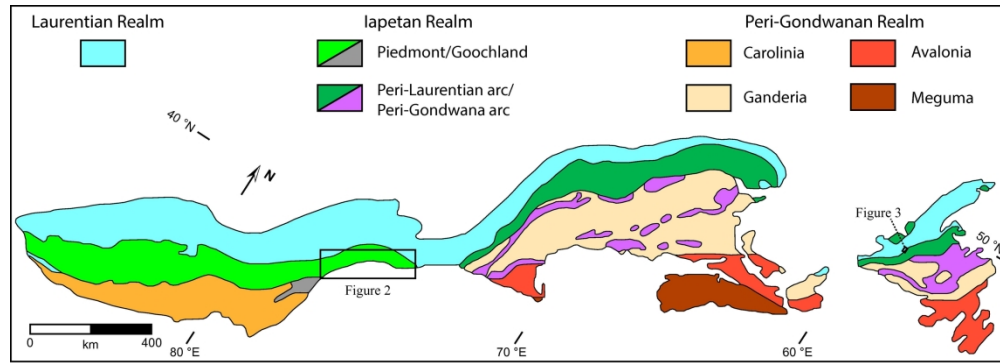


Figure 1 (Martin and Bosbyshell)

Generalized geologic map of the Appalachian Orogen. Modified from Hibbard et al. (2006).

231x119mm (300 x 300 DPI)

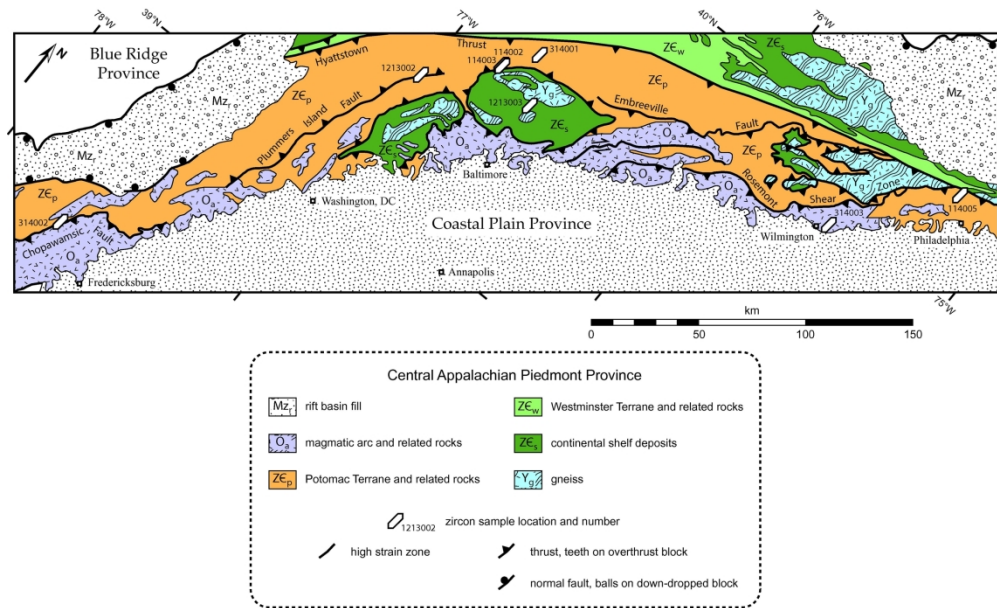


Figure 2 (Martin and Bosbyshell)

Geologic map of part of the central Appalachian Piedmont Province. Modified from Hibbard et al. (2006), Southworth et al. (2007), Hughes et al. (2014), and Martin et al. (2015).

219x163mm (300 x 300 DPI)

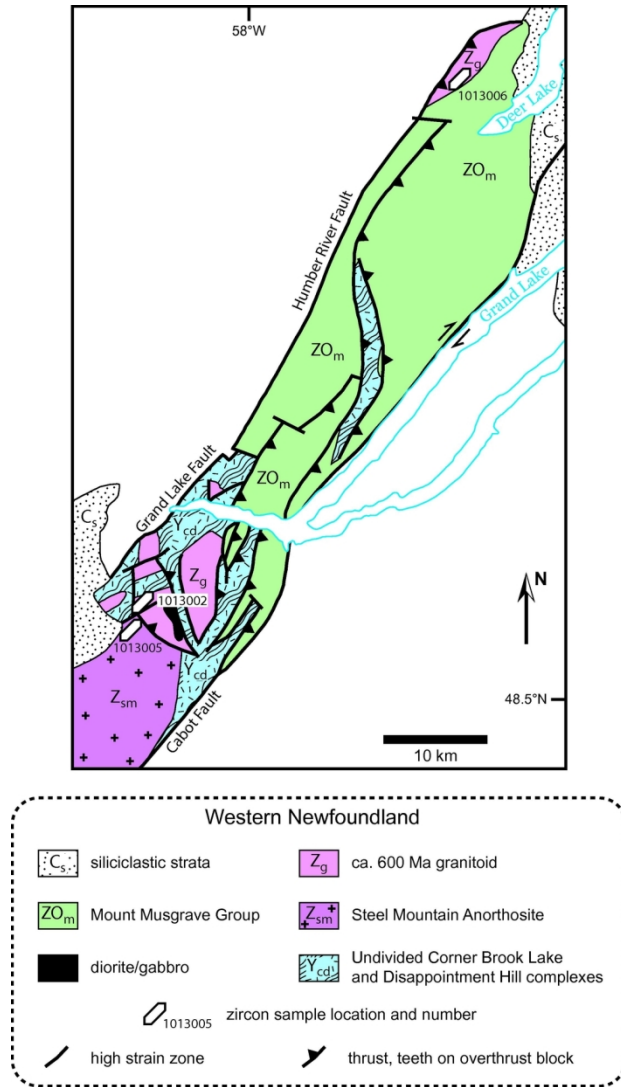


Figure 3 (Martin and Bosbyshell)

Geologic map of part of western Newfoundland. Modified from Brem et al. (2006) and Lin et al. (2013).

94x183mm (300 x 300 DPI)

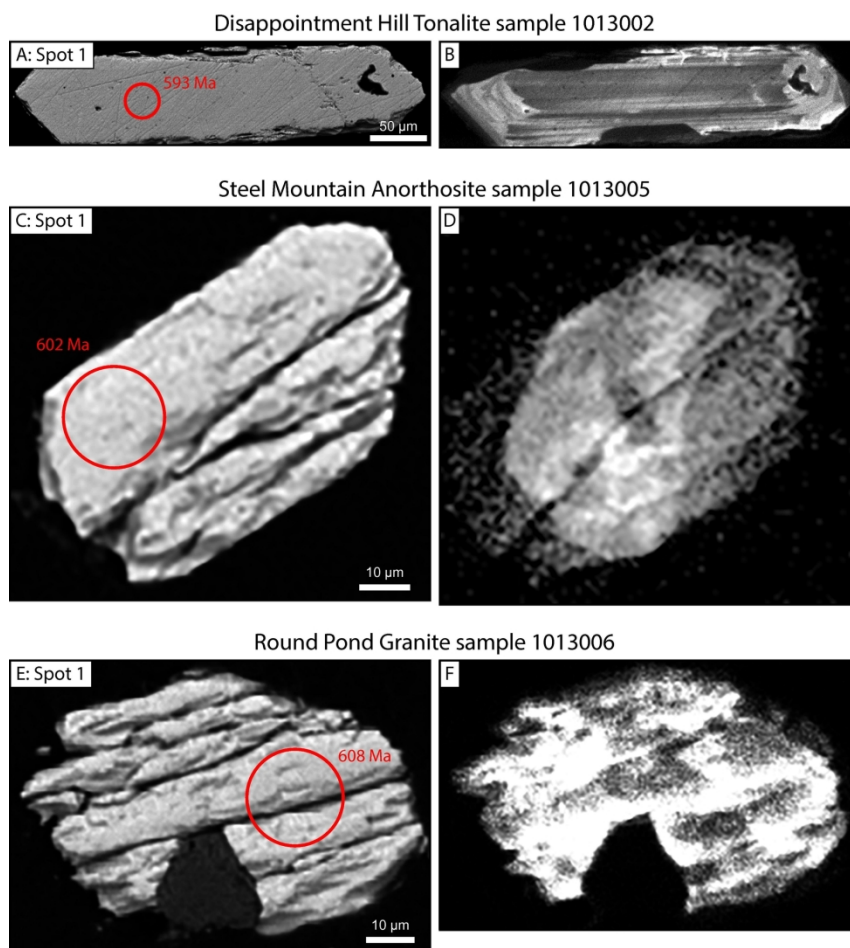


Figure 4 (Martin and Bosbyshell)

Backscattered electron (left column) and cathodoluminescence (right column) images of zircon from the three samples of western Newfoundland intrusive rocks. The circles show the locations of 20 µm-diameter laser spots that yielded the indicated $^{206}\text{Pb}/^{238}\text{U}$ ages.

154x217mm (300 x 300 DPI)

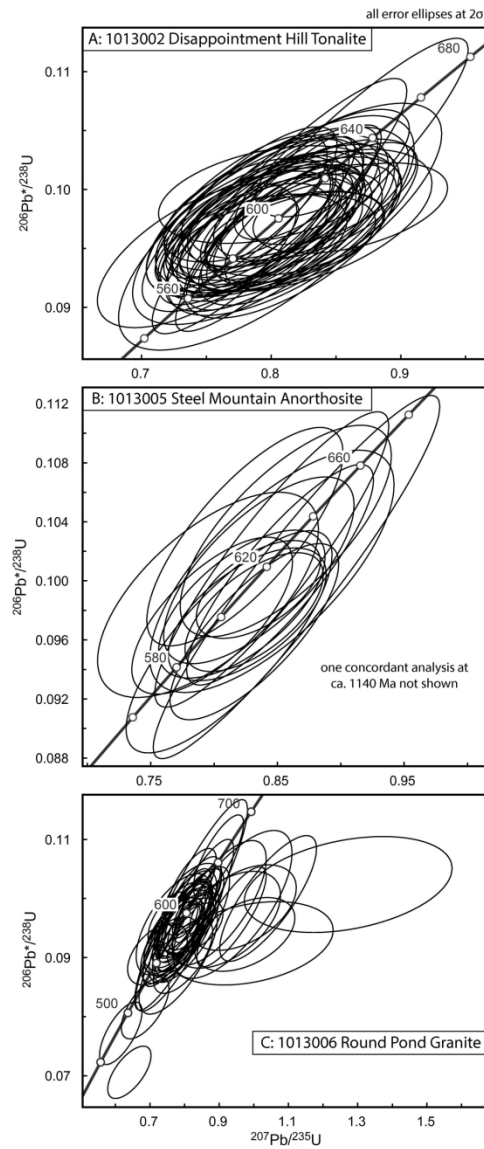


Figure 5 (Martin and Bosbyshell)

Concordia diagrams for U/Pb isotope analyses of spots in zircon from the three samples of western Newfoundland intrusive rocks.

101x253mm (300 x 300 DPI)

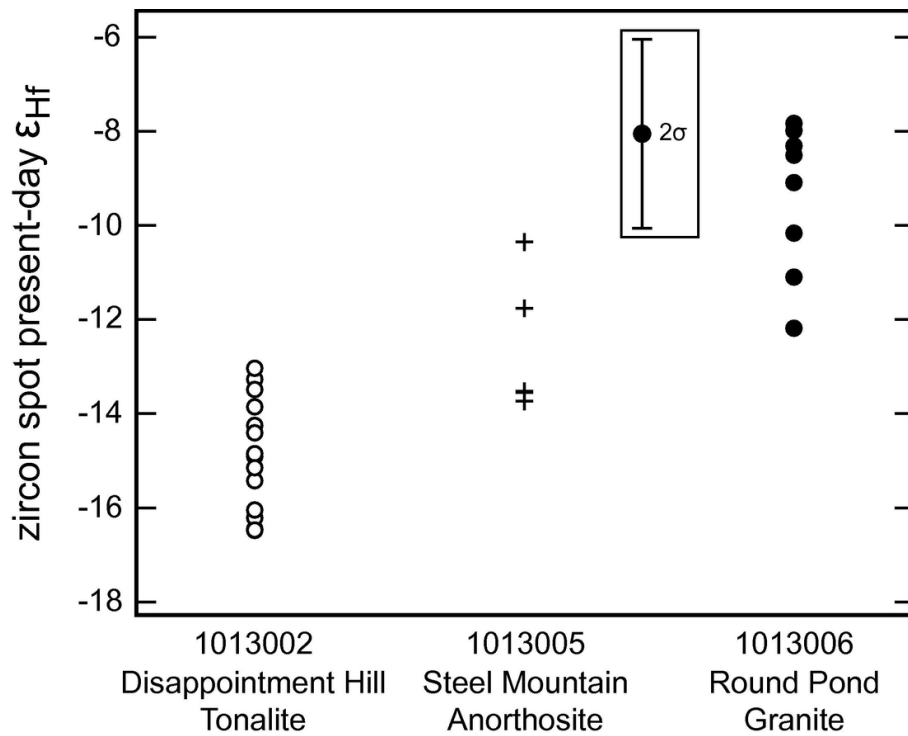


Figure 6 (Martin and Bosbyshell)

Modern ϵ_{Hf} values of spots in zircon from the three samples of western Newfoundland intrusive rocks.

94x123mm (300 x 300 DPI)

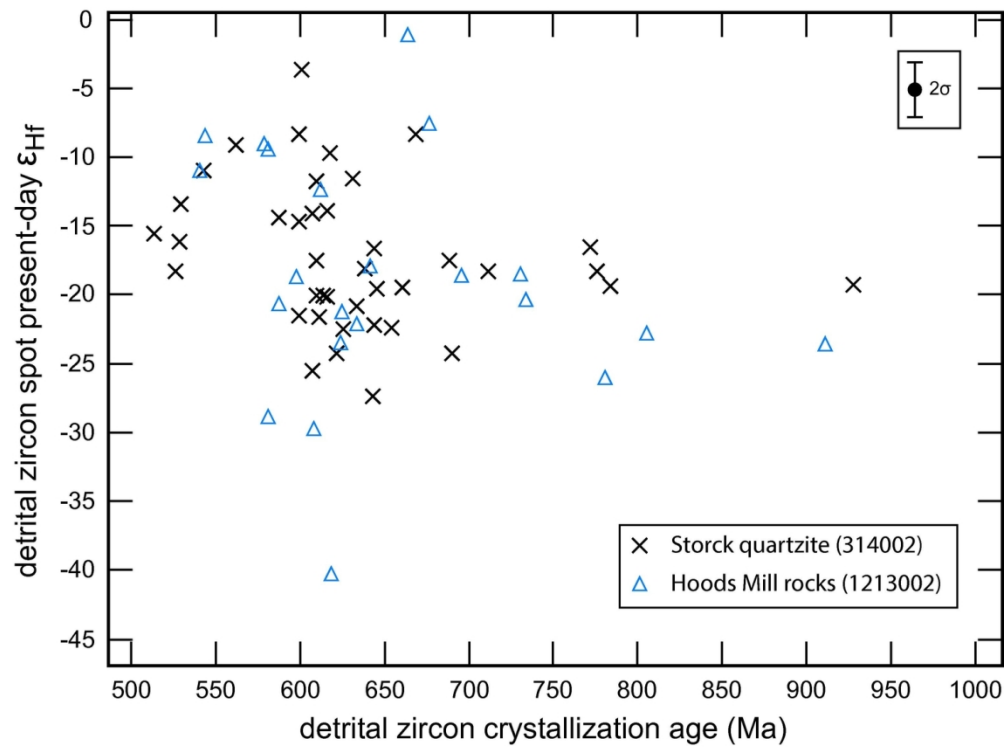


Figure 7 (Martin and Bosbyshell)

Modern ϵ_{Hf} values versus crystallization age for detrital zircon from the Storck quartzite and the Hoods Mill rocks. There is no correlation between zircon crystallization age and modern ϵ_{Hf} value.

131x157mm (300 x 300 DPI)

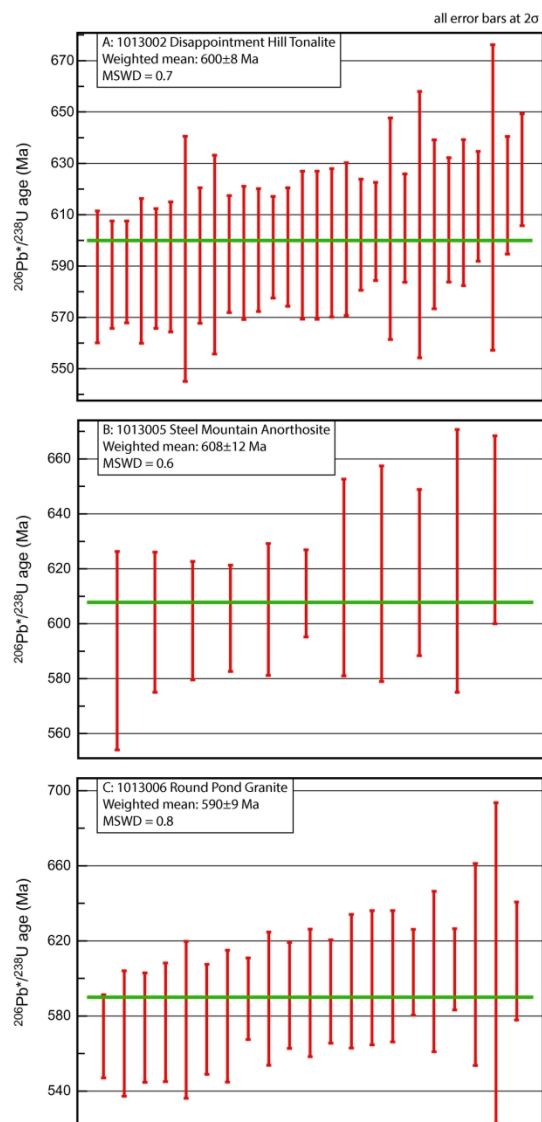


Figure 8 (Martin and Bosbyshell)

Plots of concordant, non-xenocrystic U-Pb isotope analyses (vertical red bars) from each sample of western Newfoundland intrusive rocks showing the weighted mean $^{206}\text{Pb}/^{238}\text{U}$ age (horizontal green bar). The reported uncertainty includes both measurement and systematic errors.

108x241mm (300 x 300 DPI)

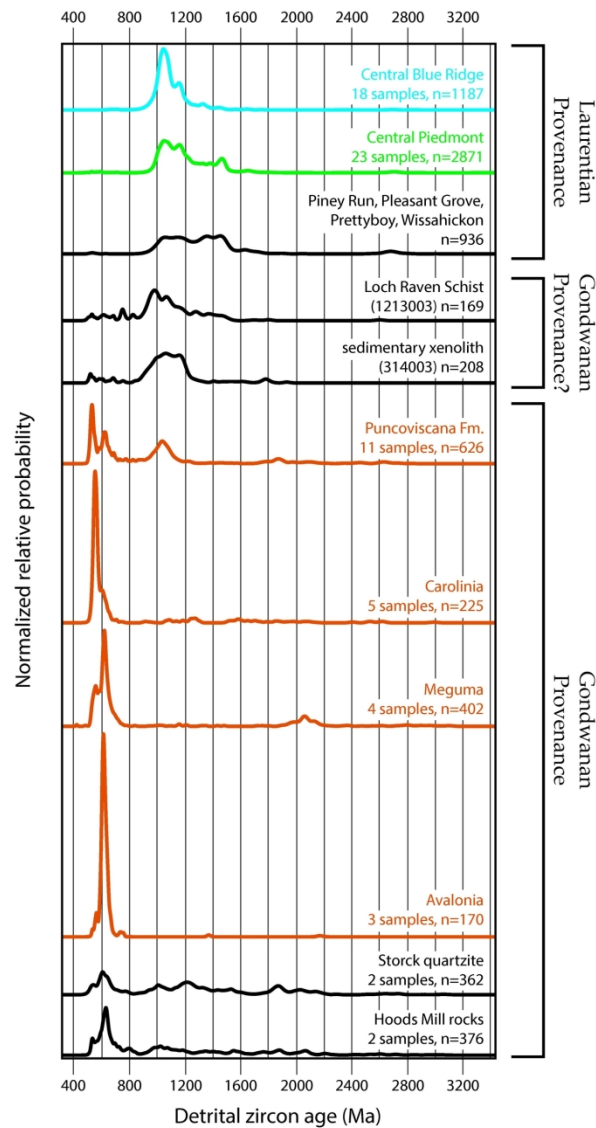


Figure 9 (Martin and Bosbyshell)

Normalized relative probability plots of detrital zircon ages from our samples compared to detrital zircon ages from other late Ediacaran-Cambrian Laurentian and peri-Gondwanan sandstone. Data were normalized so that the area under each curve is the same. Data sources and processing details are given in Table S5 and the ages and corresponding errors are in Table S6. The sample numbers for the Piney Run Formation, Pleasant Grove Schist, Prettyboy Schist, and Wissahickon Formation are 114002, 114003, 314001, and 114005, respectively.

115x236mm (300 x 300 DPI)

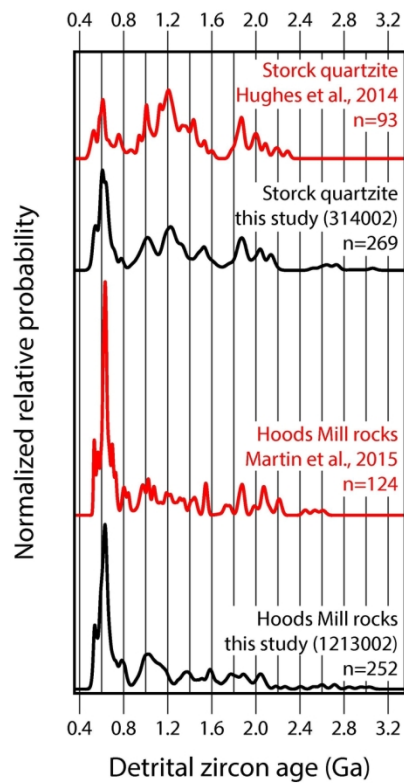


Figure 10 (Martin and Bosbyshell)

Normalized relative probability plots of detrital zircon ages from the Storck quartzite and the Hoods Mill rocks. The detrital zircon age spectra from our new samples are nearly identical to the previously-published spectra from these units. Data were normalized so that the area under each curve is the same. Data processing is described in Table S5.

67×184mm (300 × 300 DPI)

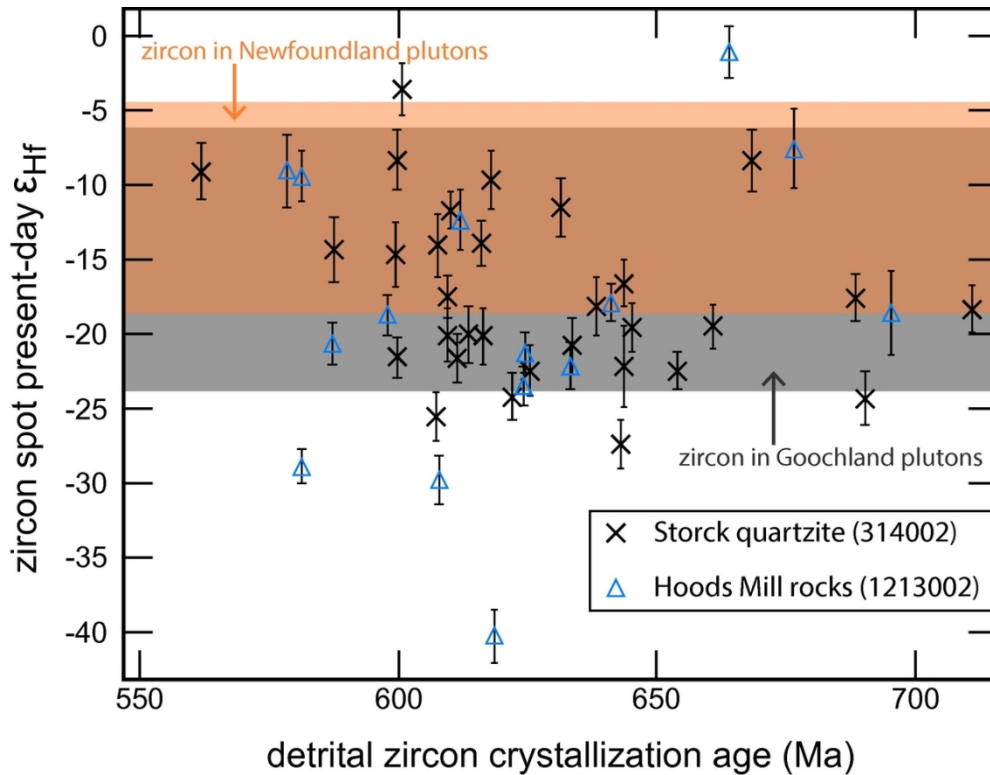


Figure 11 (Martin and Bosbyshell)

Comparison of present-day ϵ_{Hf} values of 670-580 Ma detrital zircon from the Storck quartzite and the Hoods Mill rocks with modern ϵ_{Hf} values of zircon in Neoproterozoic plutons in the Goochland Terrane and western Newfoundland. The present-day ϵ_{Hf} values of the detrital zircon extend to values both less and more negative than the zircon in the plutons, outside uncertainty. The plot shows only detrital grains with ages that overlap the age range 670-580 Ma within uncertainty. These are grains 131 to 218 in sample 314002 and 69 to 266 in sample 1213002 (Table S3). The range of ϵ_{Hf} values for the zircon in the plutons includes uncertainties. The bands of values for the plutons are shown stretching horizontally across the entire diagram to ease viewing, but the actual range of intrusion ages is 630-590 and 660-580 Ma for the western Newfoundland and Goochland plutons, respectively. ϵ_{Hf} values for the Goochland Terrane zircon from Martin et al. (2018).

108x118mm (300 x 300 DPI)